Journal of Hazardous Materials 472 (2024) 134446

Contents lists available at ScienceDirect

Journal of Hazardous Materials

journal homepage: www.elsevier.com/locate/jhazmat

Field-aged rice hull biochar stimulated the methylation of mercury and altered the microbial community in a paddy soil under controlled redox condition changes

Felizitas Boie [a], Thomas F. Ducey [b], Ying Xing [a,c], Jianxu Wang [a,d], Jörg Rinklebe [a,*]

[a] University of Wuppertal, School of Architecture and Civil Engineering, Institute of Foundation Engineering, Water and Waste Management, Laboratory of Soil and Groundwater Management, Pauluskirchstraße 7, 42285 Wuppertal, Germany
[b] US Department of Agriculture, Coastal Plains Soil, Water, Plant Research Center, 2611 West Lucas Street, Florence, SC, USA
[c] School of Chemistry and Materials Science, Guizhou Normal University, Guiyang 550002, PR China
[d] State Key Laboratory of Environmental Geochemistry, Institute of Geochemistry, Chinese Academy of Sciences, 550082 Guiyang, P.R. China

HIGHLIGHTS

- Rice hull biochar enhanced the abundance of aromatic hydrocarbon degraders.
- Biochar-derived organic matter increased microbial interactions and Hg methylation.
- MeHg content decreased without substrate input under oxidizing conditions.
- Actinobacteria and nitrogen-fixing genus *Hyphomicrobium* supported MeHg degradation.
- Microbial networks were more important than single species in Hg transformation.

GRAPHICAL ABSTRACT

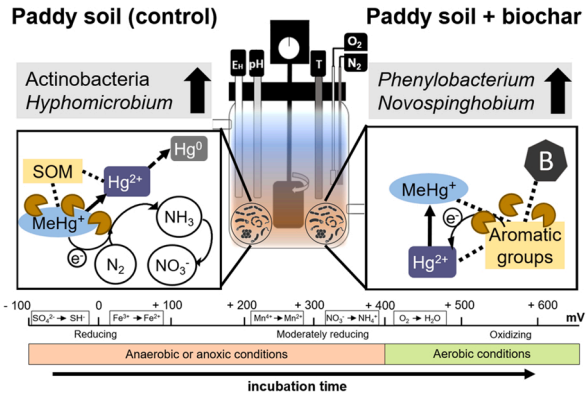

ARTICLE INFO

Keywords:
Hg methylation
MeHg demethylation
Microbial community network
Phospholipid fatty acids (PLFA)

ABSTRACT

Mercury (Hg) contaminated paddy soils are hot spots for methylmercury (MeHg) which can enter the food chain via rice plants causing high risks for human health. Biochar can immobilize Hg and reduce plant uptake of MeHg. However, the effects of biochar on the microbial community and Hg (de)methylation under dynamic redox conditions in paddy soils are unclear. Therefore, we determined the microbial community in an Hg contaminated paddy soil non-treated and treated with rice hull biochar under controlled redox conditions (< 0 mV to 600 mV) using a biogeochemical microcosm system. Hg methylation exceeded demethylation in the biochar-treated soil. The aromatic hydrocarbon degraders *Phenylobacterium* and *Novosphingobium* provided electron donors stimulating Hg methylation. MeHg demethylation exceeded methylation in the non-treated soil and was associated with lower available organic matter. Actinobacteria were involved in MeHg demethylation and interlinked with nitrifying bacteria and nitrogen-fixing genus *Hyphomicrobium*. Microbial assemblages seem more important than single species in Hg transformation. For future directions, the demethylation potential of *Hyphomicrobium*

* Corresponding author.
E-mail address: rinklebe@uni-wuppertal.de (J. Rinklebe).

https://doi.org/10.1016/j.jhazmat.2024.134446
Received 5 February 2024; Received in revised form 25 March 2024; Accepted 25 April 2024
Available online 27 April 2024

assemblages and other nitrogen-fixing bacteria should be elucidated. Additionally, different organic matter inputs on paddy soils under constant and dynamic redox conditions could unravel the relationship between Hg (de) methylation, microbial carbon utilization and nitrogen cycling.

1. Introduction

Human exposure to mercury (Hg) is a health problem worldwide. Hg exists in different forms, including bioavailable inorganic mercury (Hg^{2+}) and bioaccumulative organic mercury compounds such as methylmercury (MeHg: CH_3Hg^+). MeHg is frequently found in Hg contaminated paddy soils and can accumulate in rice plants from where it directly enters the food chain [1,2]. The daily intake of MeHg should not exceed 0.1 μg/kg body weight since it can cause severe neurotoxic diseases in the human body [3].

Increased MeHg production occurs under water level fluctuations with dynamic redox conditions which makes Hg contaminated paddy soils hot spots for Hg methylation [4-6]. MeHg is formed under anoxic conditions by microorganisms [7,8] carrying the Hg methylation genes *hgcA* and *hgcB* [9]. The *hgcAB* genes and homologues were detected in bacterial species from the phyla Proteobacteria and Firmicutes as well as Archaea [9,10]. These phyla mainly linked Hg methylation to sulfate reduction, iron reduction and fermentation as well as to methanogenesis [11-13]. Until now, only a few anaerobic bacterial species with the *hcgAB* gene pair have been identified. Likewise, correlations between expression of *hgcAB* and net Hg methylation are lacking, which potentially indicates that microbial community Hg methylation may be broader than previously suspected [14,15,5]. Putative non-methylators could indirectly support the formation of MeHg by unknown methylation pathways or other processes [16]. The genes *merA* and *merB* were found responsible for MeHg demethylation and have been detected in a broad range of microorganisms [17,18]. Hg methylation and MeHg demethylation are processes that can occur simultaneously with different net rates [19,20]. A species of the genus *Geobacter* was found to be capable of methylating Hg and demethylating MeHg [18], while species from the genus *Clostridium* and others might also play important roles in both processes [6,18].

Hg methylation and demethylation in paddy soils depends on many biochemical factors including the activity and the composition of the microbial community [21,13,2,18], but also on the concentration of total Hg and Hg species [22,23], sulfur and iron species as well as other redox sensitive compounds [2,6]. Furthermore, organic matter has binding sites for Hg controlling Hg bioavailability and affecting Hg methylation [24,25,5]. Organic matter donates electrons to the anaerobic microorganisms responsible for Hg methylation [26-28]. Therefore, organic matter inputs to paddy soils can enhance the transformation of Hg and increase MeHg contents [26-28].

Biochar is able to immobilize Hg by its binding sites and prevents the uptake of MeHg in the rice plant [1,29]. However, in Hg contaminated soils under flooding and controlled redox potential (E_H) changes, pinecone biochar showed only limited effects on Hg immobilization [30] and no effects on dissolved MeHg concentrations [31]. Rice hull biochar even increased MeHg concentrations in the solid phase of a paddy soil under flooding and controlled E_H conditions [32]. Those studies focused on regulating effects of dynamic redox conditions and biochar on Hg species. However, the influence of biochar on microbial community structure is inconsistent [33-35]. Biochar did not alter the microbial community in a paddy soil based on phospholipid fatty acid (PLFA) profiling [35], while it changed the microbial community determined by 16 S rDNA sequencing [33,34]. Biochar can - depending on the pyrolysis temperature - provide microbial communities with nutrients and available carbon and increase microbial activity [36]. A more active microbial community enhances net Hg methylation [28]. Under simulated flooding, biochar application and controlled E_H changed PLFA profiles [30,31].

However, the regulating effect of biochar on Hg (de)methylation via microbial community alteration under controlled redox conditions has been rarely studied. How biochar-derived carbon and nutrients lead to changes in microbial community structure and functions that impact Hg methylation and MeHg demethylation is an area that requires further examination. Redox condition changes could affect biochar-derived carbon and nutrients as well as a broad range of redox sensitive elements and compounds which might influence microbial-mediated Hg (de)methylation. Our specific aims were the following: (1) elucidate the reciprocal influence of Hg (de)methylation, dissolved organic carbon (DOC) and redox sensitive elements and compounds by redox-driven microbial metabolisms; (2) unravel the impact of E_H and rice hull biochar on microbial community alteration; and (3) elucidate the associations between microbial taxa and Hg (de)methylation by various statistical analyses including network analysis.

Therefore, a paddy soil treated with and without rice hull biochar was flooded in the laboratory and the E_H was stepwise increased from reducing (< 0 mV) to oxidizing (> 500 mV) conditions using an automated biogeochemical microcosm system. The soil was collected after aging in the field for three months to enable microbial adaption to biochar. MeHg, total Hg, DOC as well as redox sensitive elements and compounds (e.g. iron, manganese, sulfur, nitrate and sulfate) were measured and the microbial community was analyzed under controlled E_H by pre-set redox windows. We combined PLFA analysis and 16 S rDNA next-generation sequencing to get a comprehensive picture of the microbial community composition.

2. Material and methods

2.1. Sampling location and characterization of soil and biochar

Samples were taken from experimental paddy fields at the Wanshan Hg mining region in China (N 27° 33' 56, E 109° 13' 52), which were cultivated with rapeseed, corn and rice in rotations. The control paddy soil had no biochar application, while the treated paddy soil was amended with 72 t ha^{-1} rice hull biochar (pyrolyzed at 550 to 600 °C) using a rotary cultivator with a depth of 20 to 30 cm. The rice hull biochar aged for three months in the field before sampling. Samples of the non-treated and the biochar-treated paddy soil were taken randomly from the top layer (1 – 30 cm). The soil samples were air-dried and sieved (< 4 mm). Soil texture was characterized as a sandy loam. The content of total mercury in the paddy soil was 39.8 mg/kg (Tab. S1). The application of biochar to the paddy soil increased the total carbon content (50 g/kg compared to 25 g/kg), the total nitrogen content (3.5 g/kg compared to 3.2 g/kg) and the methylmercury content (4.3 μg/kg compared to 2.5 μg/kg). More details about the sampling site as well as the characterization of the biochar and the soil samples was done by Xing et al. [1,32].

2.2. Biogeochemical microcosm experiment

We used an automated biogeochemical microcosm (MC) system to simulate flooding and control the E_H of the paddy soils. The MC system regulated the E_H by automatically inserting N_2 (for decreasing E_H) or synthetic air/O_2 (for increasing E_H). MC glass vessels were filled with 210 g of soil and tap water in the ratio of 1:8. No additional substrate was added to be able to observe the effect of the biochar treatment. The vessels were sealed air-tight and wrapped in aluminum foil to avoid algae growth. The soil slurry was steadily stirred (between 500 and 600 rpm) to support homogeneous conditions. E_H (measured with an Ag/

AgCl electrode and standardized to the hydrogen electrode), pH and temperature were measured with electrodes (Sensortechnik Meinsberg, Germany). The system automatically monitored the E_H, pH and temperature in each MC every ten minutes using a data-logger (LogTrans 16-GPRS, UIT, Dresden, Germany). Detailed setup information for the MC system was described by Yu and Rinklebe [37]. A soil suspension volume of 80 mL was taken at each sampling point. We conducted the first sampling one hour after flooding (initial), the next sampling at the lowest E_H established in the system (for control at - 10 mV and for biochar-treated paddy soil at - 60 mV). Afterwards, we increased the E_H stepwise to predefined windows from reducing to oxidizing conditions: 0 mV, + 100 mV, + 200 mV, + 300 mV, + 400 mV, + 500 mV, + 550 mV (+ 600 mV for biochar treatment). Samples were taken at each of these redox windows, when the E_H was stable for at least 24 h. Each sample was centrifuged for 15 min (at 5000 rpm) and separated into a solid phase sample and a soil solution sample (filtration with 0.45 μm membranes) under anaerobic conditions in an anaerobic workstation (Whitley A35 Anaerobic Work Station, Don Whitley Scientific, Shipley, UK). The soil solution samples were separated into four subsample sets and analyzed for total mercury (Hg), methylmercury (MeHg), dissolved organic carbon (DOC), nitrate, sulfate as well as for further redox sensitive elements (S, Fe, Mn). The solid phase samples were analyzed for MeHg and for the microbial community. Subsamples were freeze-dried and used for PLFA extraction, DNA extraction and next-generation sequencing.

2.3. Chemical analyses of the soil solution and solid phase samples

We extracted MeHg from the solid phase samples of the initial and three redox windows (the lowest E_H with < 0 mV, 200 mV and > 500 mV) after the method of Liang et al. [38] using a mixture of $CuSO_4$--methanol. Phase separation was done with dichloromethane (CH_2Cl_2) and the extracted MeHg was then measured by cold vapor atomic fluorescence spectroscopy (CVAFS, Brooks Rand Instruments, USA).

For the analysis of dissolved total Hg and MeHg, a subsample set of the soil solution was acidified with concentrated HCl (45%). Hg concentrations were measured by a DMA-80 Hg analyzer (Milestone Srl, Sorisole, Italy) with an absolute detection limit of 0.05 ng. MeHg concentrations in the subsamples were determined in accordance with method 1630 of the U.S. Environmental Protection Agency [39]. Another subsample set of the soil solution was analyzed for dissolved organic carbon (DOC) and total dissolved nitrogen (TDN) using a C/N-analyzer (multi N/C 2100 S, Analytik Jena, Germany) as well as nitrate (NO_3^-) and sulfate (SO_4^{2-}) using an ion chromatograph (Personal IC 790, Metrohm, Filderstadt, Germany) with a detection limit of 0.03 mg/L. A third subsample set was used to measure the "average" absorbance of UV light at 254 nm by the molecules that comprise DOC in the soil solution by an UV/VIS spectrophotometer with a 1 cm path length cell (CADAS 200, Dr. Lange, Germany). The specific UV absorbance measured at 254 nm (SUVA) provides information on the aromaticity of DOC and was calculated by normalizing the absorbance to the DOC concentration after Weishaar et al. [40]. Furthermore, a fourth subsample set of the soil solution was acidified by 1% with concentrated HNO_3 (65%) and analyzed for redox sensitive elements including iron (Fe), manganese (Mn) and sulfur (S) using inductively coupled plasma atomic emission spectroscopy (Ultima 2, Horiba Jobin Yvon, Germany). Triple measurements were conducted for all chemical analyses.

2.4. Extraction and analysis of phospholipid fatty acids

PLFAs were extracted from 1 g of each of the freeze-died solid phase samples after the slightly modified method of White et al. [41] and Frostegård et al. [42]. Each sample was mixed with citrate buffer (0.15 M; pH 4), chloroform and methanol (0.9:1:2; v/v/v) which was repeated three times. The eluents were collected and extracted again using citrate buffer and chloroform. After phase separation, the liquid phase was removed by vacuum pumping and the lipid containing organic phase was concentrated. The lipid separation from the organic phase was carried out with solid phase extraction (SPE) silica columns (Bond Elut SI, 500 mg bed mass, 3 mL; Agilent; USA) only using the separated phospholipid fraction solved in methanol for further analysis. The phospholipid faction was methylated to fatty acid methyl esters (FAMEs) using methanol and toluene (1:1; v/v) and alkalized methanol. The FAMEs were extracted two times with an extraction reagent (hexane, tert-butyl methyl ether, chloroform; 2:2:1; v/v/v) and acetic acid (1 M). The extracted FAMEs were solved in hexane and tert-butyl methyl ether (1:1; v/v) and measured with a coupled gas chromatography mass spectrometry system GCMS-QP2010 Ultra (Shimadzu, Japan) equipped with a nonpolar DB-5MS GC column (60 m, 0.25 mm, 0.25 μm, Agilent, USA). Methyl nonadecanoate (C19:0) was used as an internal standard for quantitative analysis. The mass spectra were compared to an external standard containing a mixture (1:1) of 26 bacterial acid methyl esters (BAMEs; Supelco, USA) and 37 FAMEs (Supelco, USA) and to the archived mass spectra in the Lipids 1.0 Library (Chromaleont S.r.l., Italy) for determining the phospholipid fatty acids (PLFA). All PLFAs were summed up to the total PLFA ($PLFA_{tot}$) in nmol g^{-1} which is an indicator for the total viable microbial biomass [43,44]. We grouped PLFAs by their chemical binding forms as cyclopropane (CYCLO), methyl-branched saturated (MBSAT), terminally branched saturated (TBSAT), polyunsaturated (POLY), monounsaturated (MONO) and unsaturated (NSAT) fatty acids [43]. Furthermore, the abundance of these groups concerning the total PLFA was calculated in mol%.

2.5. Extraction of 16 S rDNA and next-generation sequencing

We extracted DNA from the soil samples using a phosphate buffer with 5% cetyltrimethylammonium bromide (CTAB) and a 25:24:1 mixture of phenol, chloroform and isoamylalcohol after Tatti et al. [45]. The precipitation of the nucleic acids was done with polyethylene glycol (PEG) buffer, and ice-cold 70% ethanol was used for the cleaning step. After short air-drying the nucleic acids were resuspended in ultra-pure water and measured with a micro volume UV/VIS-spectrophotometer (NanoDrop, ThermoFisher Scientific, USA). DNA amplifiability was determined by using 1.0 μL of each DNA extraction in a standard PCR reaction (25 cycles, 52 °C amplification) using bacterial primers 341 F (5' - CCTAYGGGRBGCASCAG - 3') and 806 R (5'- GGACTACNVGGGTWTCTAAT - 3') with Promega GoTaq G2 Flexi Polymerase kit (Promega Corporation, Madison, WI, USA) according to manufacturer specifications. After confirmation of successful amplification, libraries were constructed from each sample using the universal bacterial primers 515 f-Y (5' GTGYCAGCMGCCGCGGTAA - 3') and 806r Modified (5' GGACTACNVGGGTWTCTAAT - 3') which cover variable region V4 [46,47]. We used designed primers according to the Ion Amplicon Library Preparation Fusion Methodology (Life Technologies, Carlsbad, CA). We synthesized for direct-to-sequencing application by IDT (Integrated DNA Technologies, Coralville, IA, USA) with an A-adaptor, TAG Sequence, GoLay or IonXpress barcode for each bacterial specific forward primer 515 f-Y (going from 5' to 3') and the truncated P1 (trP1) adapter sequence for the 806r Modified reverse primers. Individual amplicon libraries (both forward and reverse) for bacterial community analysis were generated using the Fusion PCR library preparation methodology under the following protocol: 3 min at 94 °C to activate the enzymes, 30 s at 94 °C for denaturation (40 cycles), 30 s at 58 °C for annealing, and 45 s at 68 °C for elongation. The quantification of amplicons was done with a Qubit Fluorometer (Invitrogen, Carlsbad, CA, USA), the quality control on an Agilent 2100 BioAnalyzer (Agilent, Santa Clara, CA, USA), and the mixing of amplicons in equimolar amounts prior to sequencing on the Ion Torrent Personal Genome Machine (ThermoFisher Scientific, Carlsbad, CA, USA) according to manufacturer protocols using 316 chips. The results from sequencing were uploaded to the Ion Reporter Software v 5.2 pipeline as unaligned binary data files using the Metagenomics 16 S workflow version w1.1

with operational taxonomic unit (OTU) comparisons against ThermoFisher's curated MicroSEQ ID 16 S rDNA 500 library (v2013). This workflow has a read length filter of 150 bp, minimum alignment coverage of 90%, requires a minimum of 10 unique reads to form an OTU for inclusion in analysis, and sets genus and species cutoffs of 97% and 99%, respectively.

2.6. Quality assurance and statistical analyses

Data quality control was assured generally by blank samples, calibration with standard solutions (Merck) and triplicate measurements with defined acceptable relative standard deviation (RSD) of < 15%. Quality of Hg analysis was assured with certified soil reference materials (references GBW(E)070009 and CC580 from the Institute of Geophysical and Geochemical Exploration, China).

All statistical analyses were performed with the statistical software R [48] and Origin Pro 2023 (OriginLab Corporation, Northampton, USA). Significant differences of data mean values were calculated in R with one-way ANOVA and checked with the Tukey's HSD test. Correlation matrices were calculated using Pearson's method. We generally performed statistical analyses with relative phospholipid abundances (in mol%) and abundances of bacterial genera (in %) higher than 0.5 to avoid distortion. Principle component analysis (PCA) was conducted with the correlation matrices of the bacterial genera relative abundances differentiated into Gram-positive bacteria (Actinobacteria and Firmicutes) and Gram-negative bacteria (Proteobacteria, Bacteroidetes, Nitrospirota and Verrucumicrobia), and environmental factors (DOC, redox sensitive elements and compounds). Furthermore, we conducted a correlation-based network analysis using the Fruchterman Reingold layout algorithm. We chose only significantly positive correlations ($R^2 = 0.68$; $p < 0.05$) between bacterial genera abundances and visualized the bacterial community network with the superior phyla as well as the putative Hg methylators and demethylators found in research [17,10,18]. The size of a node for each genus was calculated based on the node degree (quantity of neighbors to a node). The PCA and the network analysis were performed and visualized with Origin Pro 2023.

3. Results

3.1. E_H, pH and redox sensitive elements and compounds

The biochar-treated paddy soil (paddy soil + biochar) showed a wider E_H range than the non-treated paddy soil (control) in the microcosm experiment (Fig. 1; Table 1). The biochar-treated soil reached the lowest E_H at - 62 mV and the highest E_H at 601 mV, while the control reached – 10 and 548 mV. No data were available between 240 h and 280 h due to an error of the data logger. The pH increased in both soils as the E_H sharply dropped to the lowest value. Thereafter, the pH stayed neutral with only slight fluctuations at 400 and 500 mV. The biochar-treated soil had a significantly lower pH varying between 6.3 and 7.3 than the control with a pH between 7.0 and 7.7. The pH of the applied biochar was 6.2 (Tab. S1).

Dissolved nitrate (NO_3^-) concentrations were low at E_H < 400 mV and increased steeply for $E_H \geq 400$ mV in both soils, while the control had significantly higher concentrations of NO_3^- at E_H 300 and 400 mV than the biochar-treated paddy soil (Table 1; Fig. S1). In the soil solution of the biochar-treated soil, iron (Fe) concentrations were significantly higher at the redox windows < 100, 300 and 400 mV than in the control. The biochar-treated soil had significantly higher manganese (Mn) concentrations in the soil solution than the control. Sulfur (S) concentrations showed no significant difference between the soils, while the control had significant higher sulfate (SO_4^{2-}) concentrations than the biochar-treated soil during the redox experiment (Fig. S1). E_H was significantly positive correlated with NO_3^- and SO_4^{2-} and significantly negative correlated with Fe and Mn in both soils (Tab. S2). In the control, E_H showed also a significantly positive correlation with S.

3.2. DOC and mercury species in the soil solution and solid phase

3.2.1. Total mercury, DOC and SUVA in the soil solution

In the control, total mercury (THg) concentrations in the soil solution were significantly higher ($p < 0.01$) at the redox windows with E_H < 200 mV than at the redox windows with E_H > 200 mV (Fig. 2). When the E_H rose from reducing to oxidizing conditions, THg concentrations in the soil solution of the control steadily decreased from 0.8 to 0.1 µg/L.

The biochar-treated paddy soil reached the highest THg concentrations in the soil solution with 1.2 µg/L under reducing conditions and showed a slight decrease to 0.8 µg/L at 100 mV. Under moderately reducing conditions, THg concentrations were slightly enhanced in the biochar-treated soil with the lowest THg concentrations under oxidizing conditions similar to the control. THg concentrations in the soil solution of the biochar-treated soil were significantly higher at all redox windows ≥ 300 mV compared to the control ($p < 0.05$). In both soils, THg concentrations in the soil solution showed a significantly negative correlation with E_H (Tab. S2). In the control, THg concentrations in the soil solution were also significantly positive correlated with DOC.

Concentrations of dissolved organic carbon (DOC) showed no significant differences between the control and the biochar-treated paddy soil considering the mean of all samplings (Table 2). However, the biochar-treated soil had significantly higher ($p < 0.001$) DOC concentrations than the control at most redox windows, except at < 0 and 300 mV (Fig. 3a). DOC concentrations had higher variations in the biochar-treated soil compared to the control with the highest DOC concentration of 40 mg/L at 100 mV and the lowest DOC concentrations of 7.5 mg/L at < 0 and 300 mV. DOC concentrations in the control were significantly higher at the redox windows ≤ 200 mV than at the redox windows ≥ 300 mV reaching the highest DOC concentrations at < 0 and 100 mV. DOC concentrations in the control were significantly negative correlated with E_H, SO_4^{2-} and S (Tab. S2). DOC concentrations in the biochar-treated soil were significantly negatively correlated with the aromaticity of DOC (SUVA).

SUVA of the biochar-treated soil was significantly higher at E_H < 0 mV with 38 m^{-1} mg^{-1} L (nearly 8-fold higher than control) and at 300 mV with 28 m^{-1} mg^{-1} L (nearly 3-fold higher than control) compared to the control (Fig. 3b). In the control soil, the SUVA was significantly increased to nearly 10 m^{-1} mg^{-1} L at 300 mV and 400 mV, while it was

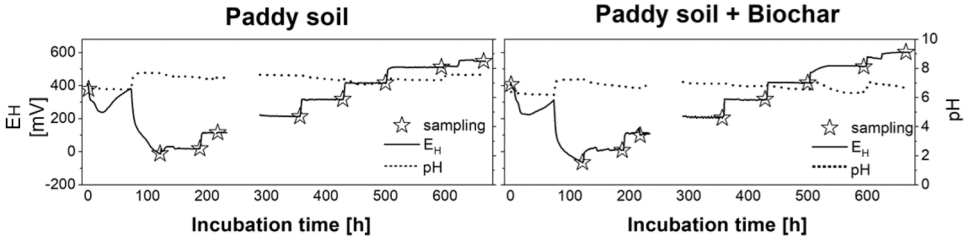

Fig. 1. Development of E_H and pH logged every 10 min during the redox experiment in the paddy soil (control) and the biochar-treated paddy soil (paddy soil + biochar).

Table 1
Chemical characterization of the sampled soil solution at different redox conditions during the experiment in the automated biogeochemical microcosm system with significant differences ($p < 0.5$) between the paddy soil (control) and the biochar-treated paddy soil (+ Biochar) in big letters (n = 3).

Chemical properties		Concentrations in the soil solution per sampling								
Control	unit	initial	2	3	4	5	6	7	8	9
E_H [6 h mean]	[mV]	392 (± 13.3)^A	-10 (± 2.8)^B	18 (± 0.4)^B	115 (± 2.5)^B	212 (± 1.0)^A	316 (± 1.0)^A	416 (± 0.6)^A	511 (± 0.6)^A	548 (± 0.2)^A
pH [6 h mean]	-	6.8 (± 0.1)^B	7.7 (± 0.0)^B	7.4 (± 0.0)^B	7.3 (± 0.1)^B	7.5 (± 0.0)^B	7.2 (± 0.0)^B	7.0 (± 0.0)^B	7.2 (± 0.0)^B	7.6 (± 0.0)^B
NO_3^-	[mg/l]	9.0 (± 1.3)^A	0.3 (± 0.2)^A	0.4 (± 0.0)^A	0.5 (± 0.1)^A	0.8 (± 0.2)^A	7.3 (± 2.0)^B	35.5 (± 5.3)^B	59.5 (± 3.6)^A	62.7 (± 3.8)^A
Fe	[mg/l]	0.09 (± 0.02)^A	1.44 (± 0.65)^A	1.70 (± 0.59)^A	1.55 (± 0.65)^A	1.08 (± 0.37)^A	0.73 (± 0.17)^A	0.69 (± 0.29)^A	0.46 (± 0.47)^A	0.12 (± 0.05)^A
Mn	[µg/l]	31.7 (± 1.2)^B	28.1 (± 3.9)^A	39.3 (± 4.1)^A	30.5 (± 2.6)^A	21.5 (± 1.5)^A	16.9 (± 2.0)^A	16.2 (± 1.3)^A	6.5 (± 0.7)^A	5.4 (± 0.2)^A
SO_4^{2-}	[mg/l]	36.5 (± 2.4)^B	30.8 (± 4.2)^B	47.3 (± 1.2)^B	24.6 (± 1.4)^B	48.0 (± 1.9)^B	48.2 (± 4.3)^B	49.5 (± 2.0)^B	55.7 (± 4.2)^B	52.4 (± 5.8)^B
S	[mg/l]	12.3 (± 1.0)^B	13.6 (± 0.8)^A	15.2 (± 1.0)^A	15.5 (± 0.2)^A	16.8 (± 0.2)^A	17.0 (± 0.2)^A	17.1 (± 0.1)^A	16.1 (± 1.1)^A	16.2 (± 1.1)^A
+ Biochar	unit	initial	2	3	4	5	6	7	8	9
E_H [6 h mean]	[mV]	413 (± 6.7)^A	-62 (± 3.6)^A	12 (± 4.0)^A	103 (± 4.1)^A	207 (± 3.6)^A	315 (± 1.9)^A	417 (± 0.9)^A	515 (± 1.5)^B	601 (± 0.4)^B
pH [6 h mean]	-	6.6 (± 0.3)^A	7.3 (± 0.0)^A	6.8 (± 0.0)^A	6.7 (± 0.0)^A	7.0 (± 0.0)^A	6.8 (± 0.0)^A	6.6 (± 0.0)^A	6.3 (± 0.0)^A	6.7 (± 0.0)^A
NO_3^-	[mg/l]	7.8 (± 0.3)^A	0.8 (± 0.3)^A	0.4 (± 0.1)^A	0.4 (± 0.0)^A	0.6 (± 0.2)^A	1.7 (± 0.6)^A	7.8 (± 2.2)^A	46.2 (± 10.7)^A	56.7 (± 14.0)^A
Fe	[mg/l]	0.34(± 0.07)^B	2.78 (± 0.97)^B	2.16 (± 0.49)^B	1.32 (± 0.04)^A	2.12 (± 0.62)^A	2.13 (± 0.29)^B	1.70 (± 0.34)^B	0.92 (± 0.57)^A	0.25 (± 0.13)^A
Mn	[µg/l]	27.6 (± 1.1)^A	64.1 (± 9.2)^B	94.6 (± 6.8)^B	78.8 (± 2.6)^B	71.0 (± 8.1)^B	83.5 (± 15.0)^B	70.2 (± 8.0)^B	37.9 (± 11.8)^B	7.2 (± 0.5)^B
SO_4^{2-}	[mg/l]	20.8 (± 1.8)^A	23.8 (± 1.0)^A	28.8 (± 0.7)^A	15.7 (± 0.6)^A	34.8 (± 2.5)^A	32.7 (± 0.4)^A	33.7 (± 2.9)^A	38.6 (± 1.8)^A	37.8 (± 0.1)^A
S	[mg/l]	9.2 (± 1.0)^A	11.6 (± 2.4)^A	11.4 (± 1.8)^A	13.4 (± 1.9)^A	13.9 (± 2.0)^A	13.0 (± 0.1)^A	12.7 (± 0.0)^A	13.0 (± 2.0)^A	14.2 (± 2.0)^A

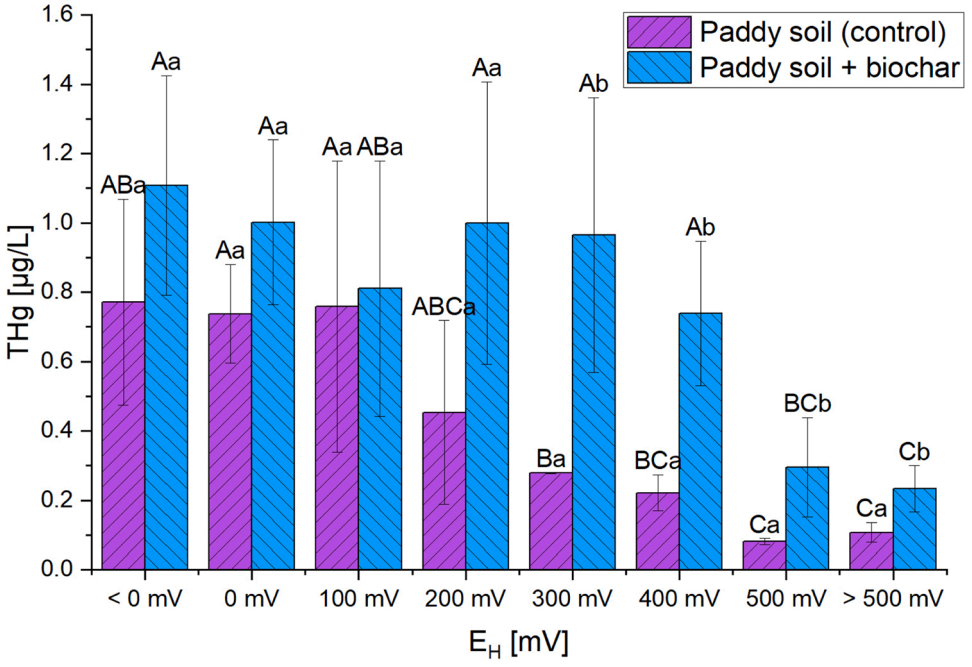

Fig. 2. Total mercury (THg) concentrations in the soil solution of the paddy soil (control) and the biochar-treated paddy soil (paddy soil + biochar) under changing redox potentials.

significantly decreased to below 5 m^{-1} mg^{-1} L under oxidizing conditions.

3.2.2. *Methylmercury in the soil solution and the solid phase*

Methylmercury (MeHg) concentrations in the soil solution showed a similar decreasing trend from reducing to oxidizing redox conditions with no significant differences ($p > 0.05$) between the control and the biochar-treated paddy soil (Fig. 4a; Table 2). The control and biochar-treated soil had the highest MeHg concentrations at 0 mV with 8.5 ng/L and 13 ng/L, respectively. Higher MeHg concentrations were measured under reducing than under oxic conditions. Lowest MeHg concentrations were measured at $E_H > 500$ mV. Paddy soil + biochar showed a steep decrease of the MeHg concentrations in the soil solution at 100 mV and a slight increase at the redox windows 200 mV and

Table 2
Comparison of the mean values for dissolved organic carbon (DOC), methylmercury (MeHg) in the soil solution and in the solid phase as well as the total concentration of phospholipid fatty acids ($PLFA_{tot}$) with small letters indicating significant differences ($p < 0.5$).

			Paddy soil (Control)		Paddy soil + Biochar	
Chemical properties	Unit	N	Mean	SD	Mean	SD
DOC	[mg/l]	9	16.47[a]	8.23	24.81[a]	10.60
$MeHg_{water}$	[ng/l]	9	4.76[a]	2.15	5.38[a]	3.40
$MeHg_{sed}$	[µg/kg]	4	5.69[a]	1.67	10.53[b]	1.01
$PLFA_{tot}$	[nmol/g]	9	66.98[a]	6.75	98.34[b]	20.34

water – soil solution; sed – solid phase

300 mV.

In the control and the biochar-treated soil, MeHg concentration in the solid phase was highest at $E_H < 0$ mV with 7.4 and 12.2 µg/kg, respectively (Fig. 4b). In the control, MeHg concentrations in the solid phase steadily decreased from reducing to oxidizing conditions with a significant difference between the redox windows < 0 and > 500 mV ($p = 0.006$). In contrast, MeHg concentrations in the solid phase of the biochar-treated soil showed no significant differences between oxidizing and reducing conditions. MeHg concentrations in the solid phase were significantly higher in the biochar-treated soil at the redox windows 200 mV ($p = 0.02$) and < 500 mV ($p = 0.003$) compared to the control. Considering the mean for all samplings, MeHg concentrations in the solid phase were significantly higher ($p = 0.01$) in the biochar-treated soil than in the control (Table 2). In the control, MeHg concentrations in the solid phase were slightly higher under oxidizing conditions than before the experiment, while they were more than doubled in the biochar-treated paddy soil (Tab. S1). Only in the control, MeHg in the soil solution and the solid phase were significantly negative correlated with E_H and MeHg in the solid phase was significantly positive correlated with DOC (Tab. S2).

3.3. The microbial community in the paddy soil and biochar-treated paddy soil

3.3.1. Total viable microbial biomass and abundances of bacterial taxa

Total viable microbial biomass ($PLFA_{tot}$) was significantly higher ($p = 0.001$) in the biochar-treated paddy soil compared to the control (Table 2). $PLFA_{tot}$ in the control slightly increased from 60 to 80 nmol/g over the whole redox experiment, except a slight decrease at the redox windows 400 and 500 mV (Fig. 5a). Biochar-treated soil had a higher variation in $PLFA_{tot}$ ranging between 60 and 120 nmol/g with the lowest value at 400 mV and the highest values at 100 and > 500 mV. We found the highest absolute concentrations for the chemical groups of unsaturated (NSAT), monounsaturated (MONO) and terminally branched saturated (TBSAT) fatty acids in both soils. Absolute concentrations for cyclopropane (CYCLO) and methyl-branched saturated (MBSAT) fatty acids were lower and polyunsaturated (POLY) fatty acids had the lowest concentrations. When calculating the concentration of those chemical

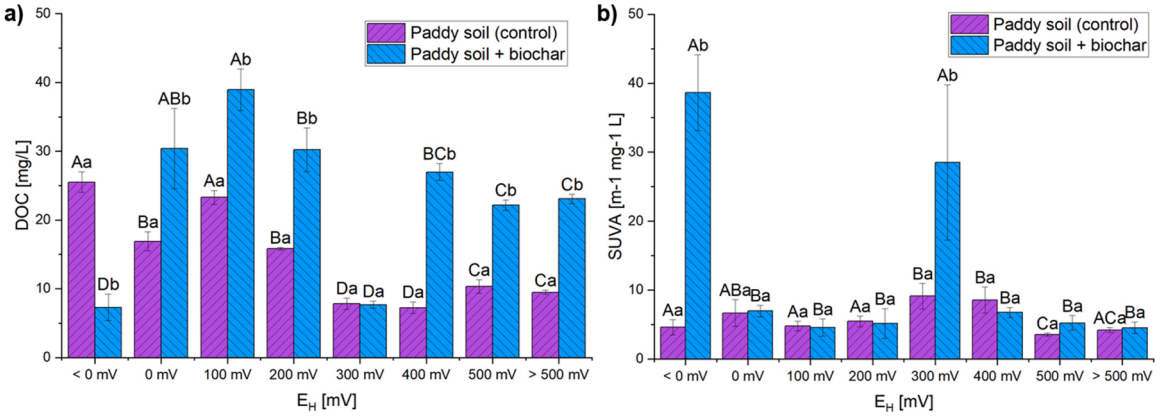

Fig. 3. a) Dissolved organic carbon (DOC) and b) aromaticity of DOC (SUVA) in the paddy soil (control) and the biochar-treated paddy soil (paddy soil + biochar) under changing redox potentials.

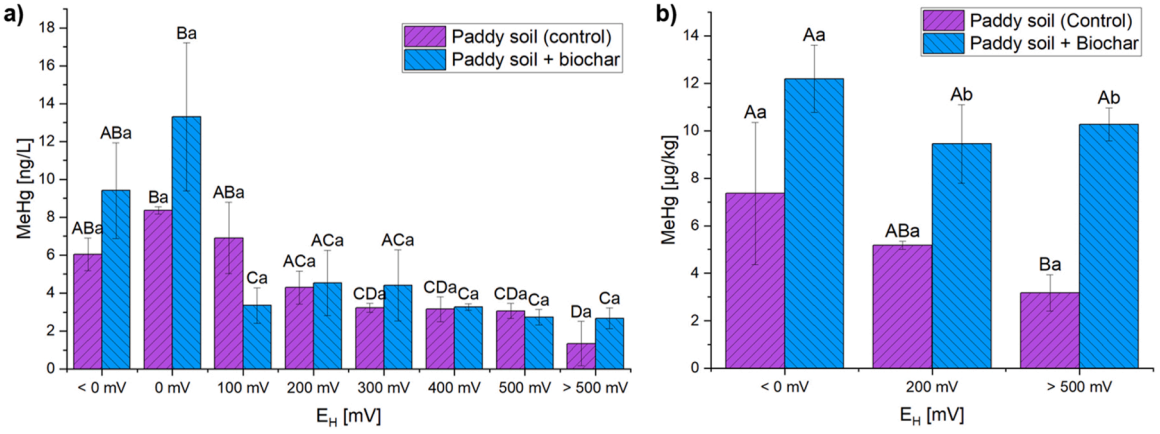

Fig. 4. a) Methylmercury (MeHg) in the soil solution and b) MeHg in the solid phase of the paddy soil (control) and the biochar-treated paddy soil (paddy soil + biochar) under changing redox potentials.

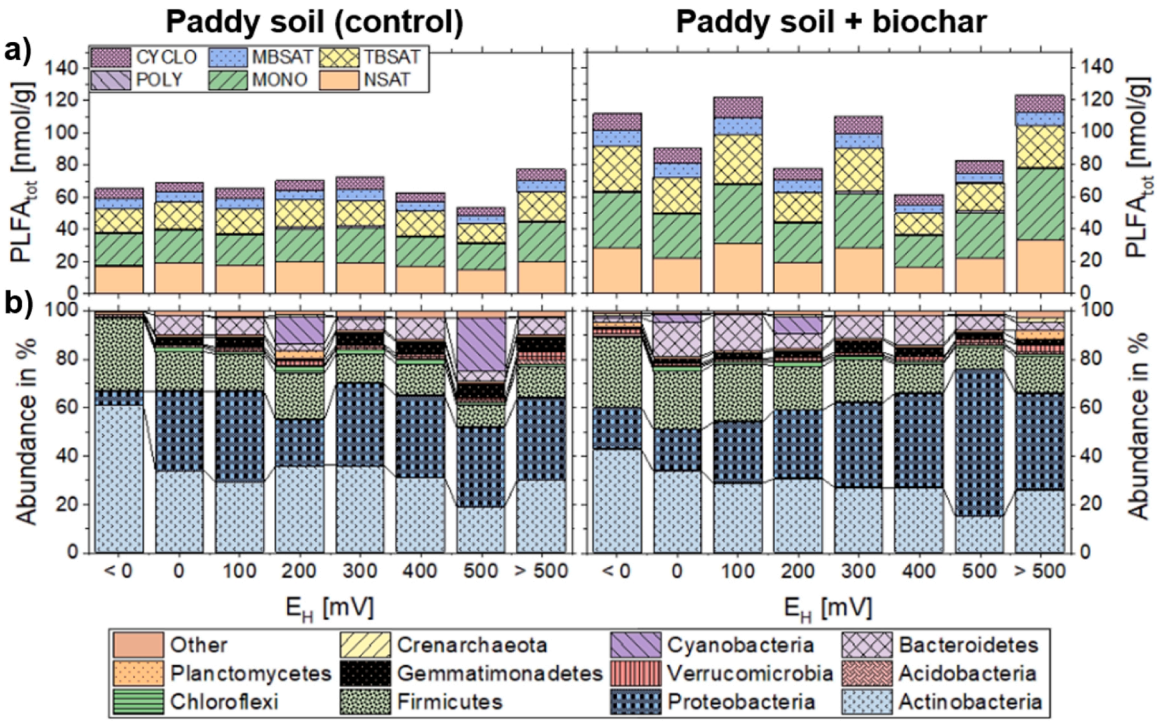

Fig. 5. a) Total phospholipid fatty acid concentration ($PLFA_{tot}$) divided in the chemical groups cyclopropane (CYCLO), methyl-branched saturated (MBSAT), terminally branched saturated (TBSAT), polyunsaturated (POLY), monounsaturated (MONO) and unsaturated (NSAT) fatty acids; b) the abundance of bacterial phyla in the solid phase taken under different redox potentials during the redox experiment.

groups in relation to $PLFA_{tot}$, we found an increasing trend for MONO and a decreasing trend for TBSAT and MBSAT from reducing to oxidizing conditions in the biochar-treated soil (Fig. S2). CYCLO decreased in the biochar-treated soil at the redox windows 500 and > 500 mV. NSAT did not change over the whole redox experiment in both soils. The relative concentrations of chemical PLFA groups showed only slight variations and no trends in the control.

The relative abundances of bacterial taxa strongly varied in the control and the biochar-treated paddy soil during the redox experiment (Fig. 5b). The bacterial phyla Actinobacteria, Proteobacteria and Firmicutes dominated in both soils with relative abundances > 60% at all redox windows and ≥ 90% at < 0 mV. In the biochar-treated soil, relative abundances of the bacterial phyla Actinobacteria and Firmicutes showed a decreasing trend from reducing to oxidizing conditions with a slight increase at > 500 mV. In contrast, the relative abundance of Proteobacteria continuously increased from 17% at < 0 mV to 40% at 500 mV and slightly decreased at > 500 mV. In the control, the relative abundance of Actinobacteria was highest at < 0 mV with 60% and lowest at 500 mV with nearly 20%, while for the other redox windows it ranged between 30% and 40%. Most genera of the Actinobacteria had significantly higher relative abundances in the control than in the biochar-treated soil, especially under moderately reducing conditions (Tab. S3; Fig. S3). The relative abundance of Proteobacteria ranged between 33% and 39% in the control, with exceptions of 8% and ~ 20% at < 0 mV and 200 mV respectively (Fig. 5b). In the control, the phylum of Firmicutes in the control had the highest relative abundance with 30% at < 0 mV. At later redox windows, the relative abundances of Firmicutes varied between 8% and 20% with a low at 500 mV. The relative abundance of Gemmatimonadetes increased from reducing to oxidizing conditions in the control, with the exception of a decrease at 200 mV. In the biochar-treated soil, the abundances of Gemmatimonadetes increased from < 0 to 300 mV and decreased from 400 to > 500 mV. Under oxidizing conditions, the relative abundance of Gemmatimonadetes was higher in the control compared to the biochar-treated soil. In contrast, the relative abundance of Bacteroidetes was higher at most redox windows in the biochar-treated soil than in the control, with exception at > 500 mV (Fig. 5b; Fig. S3). The relative abundances of the Bacteroidetes *Ferruginibacter*, *Pedobacter* and *Pontibacter* were significantly higher in the biochar-treated soil compared to the control (Tab. S3). The relative abundance of the phylum Planctomycetes was highest at 200 mV in the control, while it was highest at > 500 mV in the biochar-treated soil. The relative abundance of the phylum Verrucomicrobia was highest at > 500 mV in both soils (Fig. 5b). The relative abundance of the phylum Cyanobacteria sharply increased in the control at the redox windows 200 and 500 mV from < 1% to 10% and 22%, respectively. In the biochar-treated soil, the relative abundance of the phylum Cyanobacteria sharply increased at the redox windows 0 and 200 mV from < 1% to 4% and 8%, respectively.

In the control, Actinobacteria genera such as *Aciditerrimonas*, *Nocardioides*, *Gaiella* and *Terrimonas* showed significant positive correlations with E_H (Tab. S4). In the biochar-treated soil, Actinobacteria had no significant correlations to E_H. Genera of Proteobacteria and Verrucomicrobia were significantly, positively correlated with E_H in both soils, while most of the genera differentiated between control and biochar-treated soil, except the genus *Geobacter*. Genera of the Firmicutes such as *Bacillus*, *Clostridium*, *Sporosarcina* and *Sporacetigenium* showed significantly negative correlations with E_H in the biochar-treated soil. In the control, only the Firmicutes genus *Planococcus* was significantly, negatively correlated with E_H. Genera of Actinobacteria, Proteobacteria and Verricumicrobia were significantly, negatively correlated with DOC, while few genera of the Firmicutes were significantly positive correlated with DOC in the control. In the biochar-treated soil, DOC had no significant correlations with any bacterial taxa.

3.3.2. *Microbial community network*

The network graph of the microbial community of the control had few connections between the nodes of bacterial genera abundances, while most nodes showed close distances to each other (Fig. 6a). We further name these connections “edges”. Relative abundances of

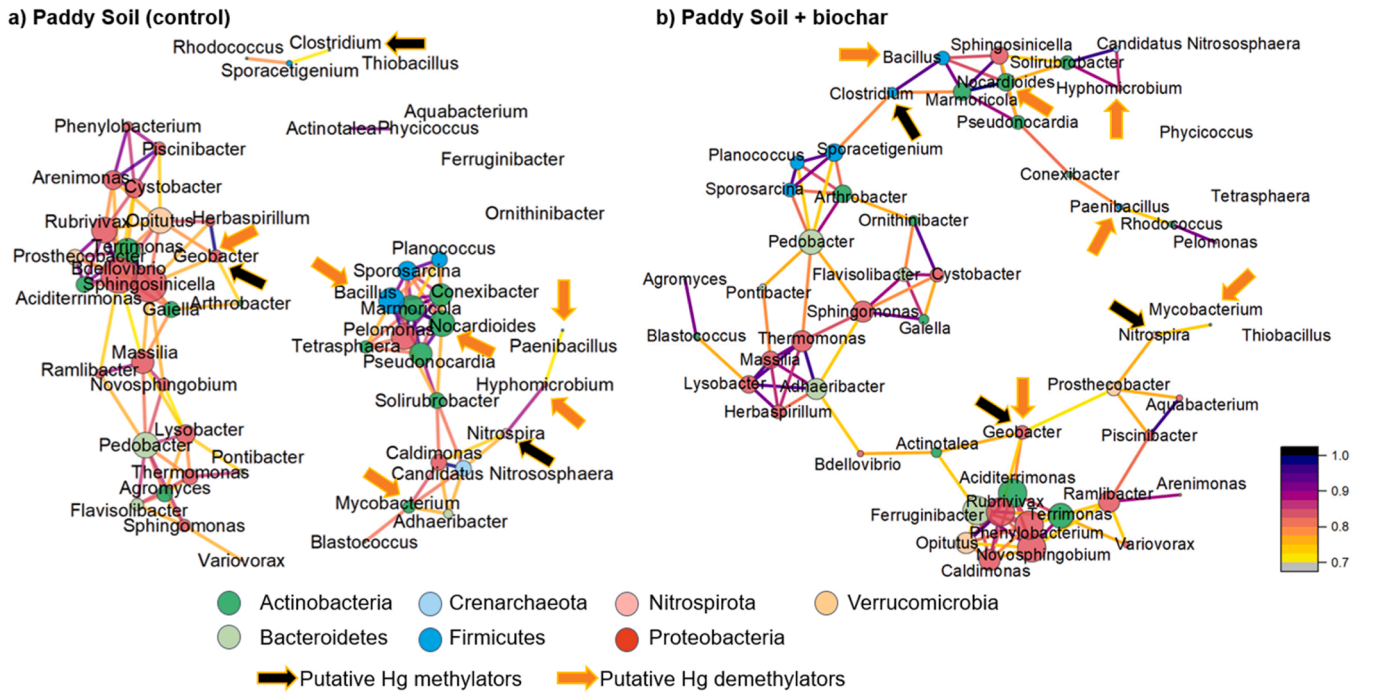

Fig. 6. Network graph of the microbial community in a) the non-treated paddy soil and b) the biochar-treated paddy soil with nodes of bacterial genera, node color representing the phyla, edges representing significantly positive correlations (yellow edges = weak significance; purple edges = strong significance), black arrows marking putative Hg methylators and orange arrows marking putative Hg demethylators.

bacterial genera in the control were clustered into three groups which were not connected by edges. One group had only very few or no edges comprising nine genera of different phyla including the genus *Clostridium* with putative Hg methylators ([24]; ORNL 2016). Another group in the control comprised most genera of the Proteobacteria. Within this group, the genera *Bdellovibrio* and *Sphingosinicella* had the biggest node size and showed many edges to other Proteobacteria, e.g. to *Geobacter* which comprises Hg methylators and demethylators. Furthermore, *Bdellovibrio* and *Sphingosinicella* were closely connected to the genera *Terrimonas*, *Aciditerrimonas* and *Gaiella* of the Actinobacteria and to the genera *Opitutus* and *Prosthecobacter* of the Verrucomicrobia. The third group was dominated by Firmicutes and Actinobacteria. This group comprised most Hg demethylating genera, with the exception of *Geobacter*. Of particular note, 3 genera of the Firmicutes, 5 genera of the Actinobacteria and *Pelomonas* of the Proteobacteria were closely clustered and had many edges of high significance. Through Actinobacteria genera, this node cluster had direct and indirect edges to a number of miscellaneous genera including *Candidatus Nitrososphaera* (Crenarchaeota), *Nitrospira* (Nitrospirota), *Mycobacterium* (Actinobacteria), *Hyphomicrobium* (Proteobacteria) and *Paenibacillus* (Firmicutes). *Hyphomicrobium* showed higher relative abundances in the control than in the paddy soil + biochar with a significant increase under moderately reducing conditions (Tab. S3; Fig. S4).

The network graph of the biochar-treated paddy soil showed more edges between the nodes then in the network graph of the control (Fig. 6b). Only two genera of the Actinobacteria did not show edges to any node, while all other genera were connected via positive correlations. Therefore, we considered the genera in this network graph as one group. *Phenylobacterium* and *Novosphingobium* of the Proteobacteria had the biggest node size and showed the closest cluster with the Proteobacteria genera *Rubrivivax* and *Caldimonas*, the Actinobacteria genera *Terrimonas* and *Aciditerrimonas*, *Opitutus* of the Verrucomicrobia and *Ferrunginibacter* of the Bacteriodetes. This cluster was closely interlinked with the genera *Geobacter* and *Nitrospira*, which contain Hg methylators. Most of the Firmicutes were closely interlinked with each other (including the genera *Clostridium* and *Bacillus*) and showed a big distance to the pre-described cluster of *Phenylobacterium* and *Novosphingobium*. In the network graph of the biochar-treated soil, the putative Hg demethylators were not as closely interlinked via edges as in the control network graph.

Few network structures were still recognizable in the biochar-treated paddy soil compared to the control, e.g. the edges between the genera *Bacillus*, *Nocardioides*, *Pseudonocardia*, *Solirubrobacter*, *Candidatus Nitrososphaera* and *Hyphomicrobium* as well as the edges between *Rubrivivax*, *Terrimonas* and *Opitutus*. Thus, most node structures, edges and correlation significances fundamentally changed after biochar application. Especially, *Phenylobacterium* and *Novosphingobium* were closer connected in the biochar-treated soil compared to the control. Furthermore, the relative abundances of *Phenylobacterium* and *Novosphingobium* were significantly higher under moderately reducing conditions in the biochar-treated soil compared to the control (Tab. S4; Fig. S5). We did not find relative abundances for genera of the sulfate-reducing Deltaproteobacteria which are known to contain proven Hg methylators.

3.4. The microbial community association with Hg, MeHg and redox sensitive elements and compounds

More bacterial genera were negatively correlated with THg and MeHg in the soil solution of the control compared to the biochar-treated paddy soil (Table 3). For instance, *Hyphomicrobium*, *Sphingosinicella* and *Opitutus* had significant negative correlations with THg concentrations in the control. Furthermore, the control showed significant negative correlations of the Proteobacteria genera *Bdellovibrio*, *Herbaspirillum* and *Rubrivivax* as well as *Opitutus* of the Verrucomicrobia with the MeHg concentrations in the soil solution. The Actinobacteria genera *Terrimonas*, *Aciditerrimonas* and *Gaiella* were also significantly, negatively correlated with MeHg concentrations in the control. The genus *Terrimonas* also had a significant negative correlation with MeHg in the solid phase of the control, while the Actinobacteria genus *Marmoricola* showed a positive correlation. In the biochar-treated soil, the Actinobacteria had no significant correlations with mercury species, neither in

Table 3
Pearson's coefficients of the bacterial genera abundances correlated with the concentrations of total mercury (THg_{water}) and methylmercury ($MeHg_{water}$) in the soil solution and methylmercury ($MeHg_{sed}$) in the solid phase of the paddy soil (control) and the biochar-treated paddy soil (+ Biochar) with significant p-values < 0.05 (*), < 0.01 (**) and < 0.001 (***).

	THg_{water}			$MeHg_{water}$			$MeHg_{sed}$		
Bacterial genera	N	Control	+ Biochar	N	Control	+ Biochar	N	Control	+ Biochar
Aciditerrimonas[1]	9	n.s.	n.s.	9	-0.81 * *	n.s.	4	n.s.	n.s.
Gaiella[1]	9	n.s.	n.s.	9	-0.69 *	n.s.	4	n.s.	n.s.
Terrimonas[1]	9	n.s.	n.s.	9	-0.80 * *	n.s.	4	-0.97 *	n.s.
Marmoricola[1]	9	n.s.	n.s.	9	n.s.	n.s.	4	0.98 *	n.s.
Adhaeribacter[2]	9	n.s.	n.s.	9	n.s.	n.s.	4	n.s.	0.999 * *
Paenibacillus[3]	9	n.s.	n.s.	9	n.s.	n.s.	4	n.s.	-0.998 * *
Planococcus[3]	9	0.79 *	n.s.	9	n.s.	0.77 *	4	n.s.	0.997 * *
Sporacetigenium[3]	9	n.s.	n.s.	9	n.s.	0.85 * *	4	n.s.	n.s.
Sphingosinicella[4]	9	-0.78 *	n.s.	9	n.s.	n.s.	4	n.s.	n.s.
Bdellovibrio[4]	9	n.s.	n.s.	9	-0.74 *	n.s.	4	n.s.	n.s.
Arenimonas[4]	9	n.s.	-0.70 *	9	n.s.	-0.84 * *	4	n.s.	n.s.
Herbaspirillum[4]	9	n.s.	n.s.	9	-0.67 *	n.s.	4	n.s.	n.s.
Hyphomicrobium[4]	9	-0.70 *	n.s.	9	n.s.	n.s.	4	n.s.	n.s.
Rubrivivax[4]	9	n.s.	n.s.	9	-0.70 *	n.s.	4	n.s.	n.s.
Opitutus[5]	9	-0.72 *	n.s.	9	-0.74 *	n.s.	4	n.s.	n.s.

[1]Actinobacteria; [2]Bacteriodetes; [3]Firmicutes; [4]Proteobacteria; [5]Verrucomicrobia

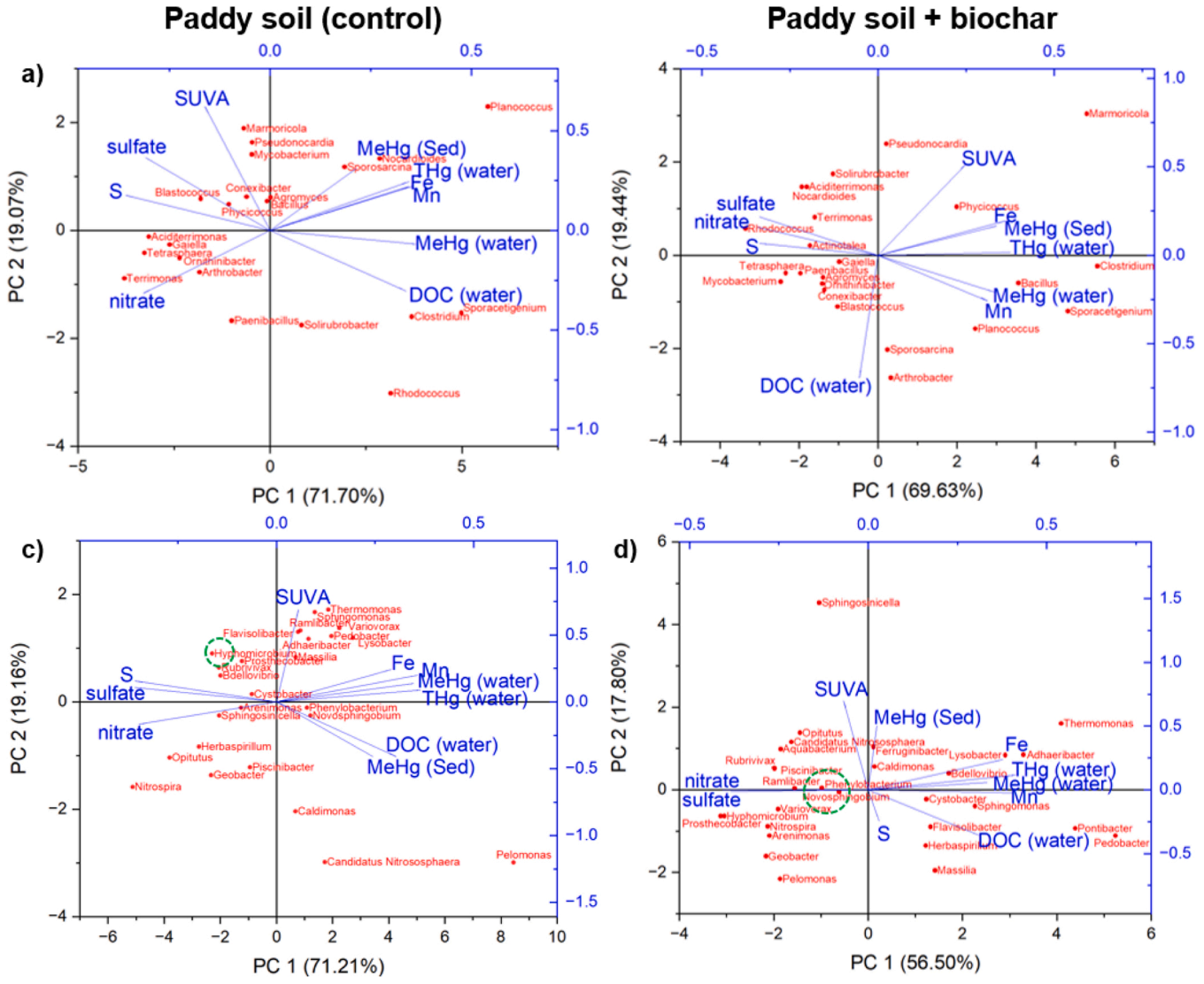

Fig. 7. Principle component analysis (PCA) for the genera of the gram-positive phyla Actinobacteria and Firmicutes (a, b) and the genera of the gram-negative phyla Proteobacteria, Bacteroidetes, Nitrospirota and Verricumicrobia (c,d) in the paddy soil (control) and the biochar-treated paddy soil (paddy soil + biochar) associated with mercury species in the soil solution (water) and in the solid phase (Sed) as well as important environmental factors (DOC, SUVA, nitrate, sulfate, S, Fe and Mn).

the soil solution nor in the solid phase. The Firmicutes genera *Planococcus* and *Sporoacetigenium* were significantly, positively correlated with MeHg concentrations in the soil solution. Generally, more significant positive correlations were shown between MeHg in the solid phase and bacterial taxa in the biochar-treated soil compared to the control. *Planococcus* (Firmicutes) and *Adhaeribacter* (Bacteroidetes) were significantly, positively correlated with MeHg concentration in the soil solid phase, while *Paenibacillus* (Firmicutes) showed a significant negative correlation. The genus *Arenimonas* had significantly, negatively correlations to THg and MeHg concentrations in the soil solution.

Most genera of the Gram-positive Actinobacteria and Firmicutes were separated by principle component 1 in both soils (Fig. 7a, b). In the control, most genera of the Actinobacteria were positively associated with the concentrations of S, sulfate, nitrate and SUVA, except the genus *Nocardioides* that was associated with MeHg concentrations in the solid phase (Fig. 7a). *Bacillus*, *Sporosarcina* and *Planococcus* of the Firmicutes were positively associated with MeHg concentrations in the solid phase, Fe and Mn. *Clostridium* and *Sporacetigenium* of the Firmicutes were positively associated with DOC. In the biochar-treated soil, *Bacillus*, *Clostridium*, *Sporacetigenium* and *Planococcus* of the Firmicutes were positively associated with the mercury species, while the genus *Sporosarcina* was closely associated with DOC (Fig. 7b). Most of the Actinobacteria genera were positively associated with concentrations of S, sulfate and nitrate.

Most genera of the Gram-negative Bacteroidetes and Verrucomicrobia were separated by principle component 1 in both soils (Fig. 7c, d). Most genera of Proteobacteria and Bacteroidetes were positively associated with SUVA in the control (Fig. 7c). The genera *Hyphomicrobium*, *Rubrivivax*, *Bdellovibrio* and *Prosthecobacter* were negatively associated with MeHg concentration in the solid phase. In the biochar-treated soil, most of the Bacteroidetes genera were positively associated with the mercury species in the soil solution and DOC (Fig. 7d). Only *Ferruginibacter* of the Bacteroidetes was positively associated with MeHg concentration in the solid phase. *Phenylobacterium* and *Novosphingobium* of the Proteobacteria were closely associated with SUVA, nitrate and sulfate concentrations as well as with MeHg concentrations in the solid phase.

Concentrations of S, sulfate and nitrate were negatively correlated to the concentrations of mercury species, Fe and Mn in both soils (Fig. 7a-d). Mercury species were closely associated with each other. MeHg concentrations in the solid phase were closer associated with the DOC concentration than with the SUVA in the control, with an inverse result in the biochar-treated paddy soil.

4. Discussion

4.1. Redox sensitive elements and compounds as electron acceptors for the microbial community

The biochar-treated paddy soil showed a wider E_H range compared to the control with the lowest E_H established at – 62 mV and the highest E_H established at 601 mV (Fig. 1). The amendment of rice hull biochar impacts the E_H range. The availability of organic matter decreases the redox potential due to the consumption of O_2 and other electron acceptors [49]. Biochar can supply organic matter and nutrients for the microbial community [36,50], which impacts the E_H range of soils amended with biochar [51].

Microbial activity is strongly influenced by the availability of organic matter as an electron donor, and electron acceptors such as O_2, NO_3^-, Mn (IV) and Fe(III) and SO_4^{2-} [27,52]. We found higher concentrations of DOC, Fe and Mn and lower concentrations of NO_3^- and SO_4^{2-} in the soil solution of the biochar-treated paddy soil compared to the control (Table 1; Fig. S1). The enhanced availability of DOC as an electron donor implies the enhanced need of electron acceptors by the microbial community to prevail their metabolisms. Microbial reduction of iron- and manganese(hydr)oxides can lead to dissolution and enhanced concentrations of Fe and Mn in the soil solution [49]. An explanation for higher Fe and Mn concentrations in the soil solution of the biochar-treated paddy soil could be enhanced microbial activity, however low pH could also lead to the dissolution of Fe and Mn [21]. The pH stayed neutral in our redox experiment with only slight fluctuations at 400 and 500 mV due to the high buffering capacity of the karstic parent material at the sampling site [1]. The reduction of Mn and Fe could have poised the E_H at > - 100 mV, while all NO_3^- was reduced in both soils, probably to ammonia [49]. NO_3^- concentrations were negligible under reducing and moderately reducing redox conditions in both soils and increased faster and steeper in the control at higher E_H compared to the biochar-treated soil (Table 1; Fig. S1). The microbial community reduces NO_3^- to ammonia under low E_H and oxidizes ammonia via nitrite to nitrate under increasing oxygen availability [53,54]. We assume, that the higher microbial activity in the biochar-treated paddy soil and carbon degradation consumed O_2 as an electron acceptor under increasing E_H. In the control, the NO_3^- concentrations already significantly increased at E_H > 200 mV, potentially due to faster oxidation of ammonia to NO_3^- by microbial activity. Enhanced microbial activity and high available Hg concentrations can increase Hg methylation [55,56,29].

The concentrations of NO_3^-, Mn, Fe and SO_4^{2-} were significantly correlated with E_H in both soils (Tab. S2). This is in accordance with the redox cascade which describes the utilization of electron acceptors after their energy gain. The reduction of NO_3^- provides similar energy gains for microbial activity and growth as the reduction of O_2, while the energy gain from Mn(IV) to Fe(III) and SO_4^{2-} reduction is gradually lower [49,57]. However, the reduced species of NO_3^-, Mn, Fe and SO_4^{2-} should be measured in future redox experiments to validate our assumptions.

Concentrations of SO_4^{2-} were lower in the soil solution of the biochar-treated soil under reducing conditions compared to the control (Table 1; Fig. S1). This could have arisen from microbial reduction of SO_4^{2-} to sulfite. Sulfate reduction was long believed to be the main driver of Hg methylation in marine, fresh-water and saltmarsh sediments [7,20], peatlands [58] and was also found to be dominant in some paddy soils [59,60]. Sulfate-reducing bacteria and methanogens would have been enhanced under highly reducing redox conditions utilizing SO_4^{2-} and CO_2 as electron acceptors [49,61]. However, SO_4^{2-} reduction or methanogenesis was of minor relevance in our study, because highly reducing redox conditions below – 100 mV were not reached. Furthermore, no known sulfate-reducing Hg methylators such as *Desulfovibrio* or *Desulfobacter* were detected in this study (Fig. S3). Sulfate-reducing bacteria were not dominant in Hg methylation in Hg contaminated wetlands [62] and also other electron acceptors were linked with Hg methylation. Previous analysis of the Hg contaminated paddy soils originating from the Wanshan mining site (same site as our paddy soils) revealed that iron-reducing bacteria and methanogens dominated Hg methylation instead of sulfate reducers [12]. Also, in boreal wetlands, Hg methylation was predominantly connected to Fe reduction [63]. Highly reducing redox conditions such as those found in sediments, peatlands and some paddy soils are favorable for sulfate-reducing and methanogenic Hg methylators when sufficient amounts of SO_4^{2-} are available [58]. However, the E_H of paddy soils depend on the soil texture, microbial community and the cultivation system, e.g. paddy soils with crop rotation and shorter cultivation periods could prevail moderately reducing redox conditions [53]. This would favor microbial activity coupled mainly to NO_3^-, Fe and Mn reduction. In the biochar-treated paddy soil with prior crop rotation, a short flooding period of three month and a coarse soil texture, the E_H poised at > - 100 mV. Therefore, microbial Hg (de)methylation was most likely linked to the reduction of the electron acceptors NO_3^-, Mn and Fe, while the reduction of SO_4^{2-} was only of minor relevance.

4.2. Biochar as electron donor for Hg methylation

In both soils, THg concentrations decreased from reducing to oxidizing redox conditions, while the biochar-treated paddy soil had

significantly higher concentrations of available THg at the redox windows with $E_H \geq 300$ mV compared to the control (Fig. 2). THg in the soil solution was significantly, negatively correlated to E_H in both soils (Tab. S2). This was in line with other studies on flooded soils and Hg methylation in automated biogeochemical microcosm systems [30,32]. Positive correlations between DOC and Hg species in the soil solution were explained by Hg binding sites of DOC [21,31]. We also found significantly positive correlations between THg and DOC in the control (Tab. S2). The biochar-treated soil showed no significant correlations between THg and DOC. On the one hand, the biochar-treated paddy soil showed higher concentrations of dissolved Mn and Fe, which were found to increase Hg mobilization [32]. On the other hand, the rice hull biochar probably provided stronger binding sites for Hg than the DOC from the paddy soil. Biochar contains aromatic functional groups as binding sites which increase Hg immobilization, while higher pyrolysis temperatures enhance the aromaticity of biochar [29,30]. Rice hull biochar was pyrolyzed under high temperatures and is rich in aromatic carbon [32]. The biochar-treated paddy soil had significantly higher concentrations of DOC at most redox windows compared to the control (Fig. 3a). Furthermore, it showed an increase in the DOC aromaticity at the redox windows with $E_H < 0$ and 300 mV (Fig. 3b). The rice hull biochar in this study aged for three months in the field and was thus exposed to changing environmental conditions and biogeochemical processes. Biochar aging includes microbial degradation which can result in the disconnection of aromatic groups due to oxidation at the break points which can be high during the first two month of incubation [64]. Flooding cycles promote biochar aging which can lead to the release of Hg from the binding sites of biochar [29]. We assume that biochar-derived organic matter was partially degraded and aromatic functional groups were attacked by the microbial community during the redox experiment. The degradation of these aromatic functional groups could have led to the additional release of biochar-derived Hg-DOC complexes. Thereby, the concentrations of THg and DOC were increased under moderately redox conditions in the biochar-treated soil. Low molecular Hg-DOC complexes can increase the availability of Hg for the microbial community [21,27]. Hg-DOC complexes could have provided electron donors as well as microbial available Hg stimulating the Hg methylation under moderately reducing to oxidizing conditions in the biochar-treated paddy soil.

DOC decreased with increasing E_H in both soils (Fig. 3a). The decrease of DOC could be explained by complexation of DOC with Fe and Mn [6] or by microbial consumption and degradation of DOC under oxidizing conditions [49].

MeHg concentrations in the soil solution showed no significant differences in both soils (Fig. 4a). DOC and MeHg in the soil solution had no significant correlations in both soils (Tab. S2). Other studies showed that DOC and MeHg were stronger correlated than DOC and THg [21,32]. In the control, MeHg in the solid phase was significantly positive correlated with DOC (Tab. S2). This could be explained by intensive Hg transformations. We observed steadily decreasing MeHg concentrations in the solid phase from moderately reducing to oxidizing conditions in the control (Fig. 4b). MeHg demethylation probably exceeded the methylation of Hg in the control. This could be explained by a lower activity of Hg methylators [27] or reductive demethylation of aerobic bacteria comprising the *mer*-genes [17,63]. Processes of Hg methylation and MeHg demethylation can appear simultaneously in paddy soils and control the net Hg formation [18,19]. Furthermore, MeHg could be used by the microbial community as electron donor [17]. We hypothesize that the low availability of organic carbon as electron donors could have suppressed Hg methylation on the one hand by a lower activity of Hg methylators. On the other hand, it might have supported MeHg demethylation by using it as electron donors. It would have led to a higher MeHg demethylation than Hg methylation rate in the control.

4.3. Microbial community alteration by EH and biochar

MeHg concentrations in the solid phase were significantly higher in the biochar-treated paddy soil compared to the control (Fig. 4b). Furthermore, $PLFA_{tot}$ in the biochar-treated soil was also higher than in the control (Fig. 5a). Low available organic matter could have restricted microbial growth in the control, while the addition of biochar could have resulted in the stimulation of microbial growth. Biochar can provide nutrients bound by the large surface area and has a porous structure which makes it a favorable habitat for microorganisms [36,64]. The application of substrates (organic matter or biochar) provides labile carbon and enhanced the microbial activity [27,52]. High available Hg concentrations and increased microbial activity enhance Hg methylation [55,56,29]. However, the reported impacts of biochar on microbial community structure have been inconsistent [33-35]. In this study, rice hull biochar shifted the relative abundances of bacterial taxa (Fig. 5b) from high relative abundances of Firmicutes under reducing conditions to high relative abundances of Proteobacteria under increasing E_H. The biochar-treated paddy soil showed high relative abundances of Firmicutes, Proteobacteria and Bacteroidetes. These bacterial phyla mainly favor higher substrate availability [65]. In contrast, the control showed higher relative abundances of Actinobacteria and Gemmatimonadetes than the biochar-treated paddy soil. Genera of these bacterial phyla are more competitive under low available substrate conditions [66,52,67]. Therefore, the shift in the microbial community structure in the biochar-treated soil was potentially triggered by biochar-derived organic matter. The relative abundance of Firmicutes was high under reducing conditions and decreased under increasing E_H in both soils (Fig. 5b). Many genera of the Firmicutes phylum are obligate anaerobic fermenters [68] and carry homologues of *hgcAB* for Hg methylation [10,63]. Therefore, genera of the Firmicutes were probably involved in methylating Hg and increasing the MeHg in the solid phase under reducing conditions. Otherwise, Firmicutes could have provided easily available substrates to other Hg methylators by producing organic acids due to fermentation. These fermentation products (e.g. acetate, lactate) were utilized by known Hg methylators as *Geobacter* from the phylum Proteobacteria [63]. We assume that the rice hull biochar regulated microbial growth measured by $PLFA_{tot}$ and altered the microbial community composition. These changes in the microbial community combined with an increased availability of Hg and DOC stimulated Hg methylation and enhanced the MeHg concentrations in the solid phase of the biochar-treated soil.

4.4. Changed interactions of the Hg (de)methylating microbial community by biochar

The microbial community network graphs of the control and the biochar-treated paddy soil partly showed similar clustering between bacterial genera (Fig. 6a and b). However, the application of rice hull biochar affected correlation significances, node distances and edges. Biochar provides carbon and nutrients, a large surface area, porous structure and thus, a favorable microbial habitat [36]. We assume that these characteristics promoted a stronger connected microbial community network in the biochar-treated soil compared to the control.

The rice hull biochar induced a clustering of *Phenylobacterium* and *Novosphingobium* with *Rubrivivax* and *Caldimonas* of the Proteobacteria as well as *Aciditerrimonas* and *Terrimonas* of the Actinobacteria (Fig. 6b). The genera *Phenylobacterium* and *Novosphingobium* can degrade aromatic hydrocarbons [69,70] and *Phenylobacterium* has been demonstrated to be enhanced in soils after addition of high temperature biochar [52] as well as after wildfires [71,72]. *Aciditerrimonas* might also utilize pyrolyzed organic matter, because it was found with dominant abundances in peatlands after wildfire [73]. *Rubrivivax* can degrade aromatic hydrocarbons [74] and participates in the shuttling of electrons similar to *Caldimonas* [75]. We assume that *Phenylobacterium* and *Novosphingobium* were primarily involved in degrading the aromatic functional groups of

the rice hull biochar. These degradation products can be used by Hg methylators when converting inorganic Hg to MeHg [7]. The *Phenylobacterium* and *Novosphingobium* cluster showed close connections to the Hg methylators *Geobacter* and *Nitrospira* (Fig. 6b). The abundance of *Phenylobacterium* and *Novosphingobium* was significantly higher under moderately reducing conditions in the biochar-treated soil compared to the control (Fig. S5), while at the same time THg and MeHg were slightly increased in the soil solution (Fig. 2; Fig. 4a). We suggest that particulate Hg-DOC complexes went into the soil solution, when the aromatic functional groups of the rice hull biochar were attacked by the aromatic hydrocarbon degraders *Phenylobacterium*, *Novosphingobium* and *Rubrivivax* of the Proteobacteria as well as *Aciditerrimonas* of the Actinobacteria. We hypothesize that *Geobacter* and *Nitrospira* could have interacted with these aromatic hydrocarbon degraders and transformed the bioavailable Hg from the Hg-DOC complexes to MeHg using the DOC as electron donor. *Geobacter*, *Ramlibacter*, *Piscinibacter*, *Aquabacterium* and *Prosthecobacter* had many significantly positive correlations with the *Phenylobacterium* and *Novosphingobium* cluster and were significantly positive correlated with E_H (Tab. S4). We assume that the *Phenylobacterium* and *Novosphingobium* cluster was more active under moderately reducing to oxidizing redox conditions suppressing MeHg demethylation.

Most genera of the Firmicutes were significantly, negatively correlated with E_H (Tab. S4) and dominated under reducing redox conditions in the biochar-treated soil (Fig. S3). Species from the genus *Clostridium* inherit homologues of *hgcAB* and can probably methylate Hg ([24]; ORNL 2016). The abundance of *Clostridium* was positively associated with MeHg concentrations in the solid phase (Fig. 7b). Therefore, we assume that *Clostridium* was involved in Hg methylation in the biochar-treated soil. *Planococcus* and *Adhaeribacter* were significantly positive correlated with MeHg concentrations in the solid phase (Table 3). Both genera were indirectly connected to Hg methylators *Geobacter* and *Clostridium* and probably supported Hg methylation. *Paenibacillus* was significantly, negatively correlated with MeHg concentrations in the solid phase (Table 3). In the network graph, *Paenibacillus* had few edges without close connections to other genera which might have restricted MeHg demethylation. We assume that intense interactions between genera of different phyla enabled the exchange of organic matter and electrons. The activity of Hg methylators decreased when less electron donors were available [27]. Here, electron donors were available due to microbial attack on biochar and biochar-derived organic matter, which stimulated Hg methylators. This finding demonstrates the importance of microbial community interactions over the activity of a single microorganism in Hg methylation.

In the control, the microbial community network graph showed less correlations and the microbial community was mainly divided into two groups (Fig. 6a). In one group, *Sphingosinicella* and *Bdellovibrio* had the biggest node size and were closely clustered with nearly all other genera of the Proteobacteria. *Sphingosinicella* comprises species with heavy metal resistance which can participate in the degradation of recalcitrant carbon [76,77]. Species of *Bdellovibrio* prey on other Proteobacteria [78], which could be an explanation for the clustering with many genera of the Proteobacteria in the network graph. Both genera could potentially generate available organic matter for other bacteria. Genera in this cluster such as *Opitutus* (Verrucomicrobia), *Rubrivivax*, *Herbaspirillum*, *Bdellovibrio* and *Sphingosinicella* (Proteobacteria) as well as *Aciditerrimonas*, *Gaiella* and *Terrimonas* (Actinobacteria) were significantly, negatively correlated with THg and MeHg in the soil solution (Table 3). *Terrimonas* showed significant negative correlations to MeHg in the soil solution and in the solid phase. *Geobacter* was closely connected to all these genera (Fig. 6a). The genus *Geobacter* contains species that are able to methylate Hg and demethylate MeHg, while MeHg could be used as electron donor by MeHg demethylators [17]. We hypothesize that *Geobacter* methylates Hg, when available electron donors are provided and demethylates MeHg under electron donor limitations. This hypothesis needs to be proven in further studies.

In the control, another group of the microbial community network was dominated by genera of the Actinobacteria. The Actinobacteria cluster was closely connected with putative MeHg demethylators such as *Nocardioides*, *Paenibacillus*, *Mycobacterium* and *Bacillus* (Fig. 6a). Therefore, we suggest that genera of the Actinobacteria participated in or supported Hg demethylation in our study. Zhou et al., [18] found associations of Actinobacteria with Hg demethylators in paddy soils. Actinobacteria are: i) adapted to low substrate concentrations; ii) they can deal with complex organic matter as cellulose and in addition; iii) the demethylation gene *merA* was detected in species of the Actinobacteria [18,52]. We assume that MeHg demethylation by Actinobacteria occurs under the limitation of easily available substrates as in our non-treated paddy soil.

Hyphomicrobium was significantly, positively correlated with *Paenibacillus* and *Nitrospira* as well as indirectly connected to *Nocardioides* and *Mycobacterium*. It was negatively correlated with total Hg concentration (Table 3) and negatively associated with MeHg concentrations in the solid phase (Fig. 7c). *Hyphomicrobium* was not stated as a MeHg demethylator yet, although it is known for comprising many methylotrophs and species with the demethylation gene *merA* [60]. Furthermore, a microbial community network demonstrated significant, positive correlations of *Hyphomicrobium* with Hg demethylators in paddy soils [18]. Therefore, we hypothesize that *Hyphomicrobium* supports the demethylation of MeHg. Furthermore, like the MeHg demethylators *Mycobacterium* and *Paenibacillus*, *Hyphomicrobium* is involved in nitrogen fixation [79-81]. The genera *Hyphomicrobium*, *Mycobacterium* and *Paenibacillus* were directly linked to *Candidatus Nitrososphaera*, *Nitrospira*, *Caldimonas* and *Adhaeribacter*. *Adhaeribacter* from Bacteroidetes also comprises nitrogen fixing bacteria, while *Candidatus Nitrososphaera*, *Nitrospira* and *Caldimonas* can oxidize ammonia and nitrite [75,82]. Therefore, we posit that the demethylation of MeHg could be linked to nitrogen fixation and nitrification under oxidizing conditions in the control.

In contrast, NO_3^- was significantly lower in the biochar-treated soil and microbial nitrification might have been suppressed. Biochar compounds can deactivate enzymes involved in nitrification [52]. Another explanation might be the use of O_2 as the strongest electron acceptor for the degradation of biochar-derived organic matter. Both could have led to a lower nitrification rate. Concerning our previous assumption, a lowered nitrification rate would decrease microbial MeHg demethylation leading to higher MeHg concentrations in the solid phase of the biochar-treated soil.

Different microbial assemblages were associated with Hg methylation and MeHg demethylation in the rice-soil interface [4] and the microbial community network in different paddy soils revealed strong correlations between MeHg demethylators [18]. Even putative non-Hg methylators could play an important role in MeHg production in paddy soils due to unknown Hg methylation pathways or syntrophic relationships with Hg methylators [16].

We suggest that interactions between different genera (e.g. Actinobacteria, Firmicutes, Proteobacteria, Bacteroidetes, Nitrospirota and Crenarchaeota) occurred in our study, which were probably more important than single species in regulating Hg methylation and MeHg demethylation. Our results revealed distinct microbial assemblages potentially involved in MeHg production and Hg demethylation. Hg methylation in the biochar-treated soil was stimulated by biochar-derived organic matter, which led to a microbial community alteration with higher abundances of aromatic hydrocarbon degraders. In the control under low organic matter availability, mainly Actinobacteria associated with nitrogen-fixing and nitrifying bacteria were involved in MeHg demethylation.

5. Conclusions

Our overall aim was to elucidate the effect of biochar and dynamic redox conditions on Hg (de)methylation and the microbial community alteration. This study further unraveled the manifold interactions in the

microbial community that influence Hg methylation and MeHg demethylation. We recommend to consider Hg (de)methylating microbial assemblages instead of focusing on single species. Hg methylation and the demethylation of the highly toxic MeHg are complex processes controlled by the bioavailable Hg and the microbial community, which is dependent on DOC as electron donor and on electron acceptors (e.g NO_3^-, Fe, Mn and SO_4^{2-}), both impacted by E_H. The application of rice hull biochar increased the abundance of aromatic hydrocarbon degrading Proteobacteria such as *Phenylobacterium* and *Novosphingobium* in the microbial community. These genera probably attacked aromatic functional groups of the rice hull biochar. Thereby, bioavailable Hg-DOC complexes were increased promoting the activity of Hg methylating bacteria. The microbial degradation of functional groups of biochar during aging could enhance the formation of MeHg reducing the effectiveness of biochar for remediation. Therefore, further studies are needed to unravel the relationship between microbial Hg methylation and the utilization of biochar-derived Hg-DOC complexes due to biochar aging under dynamic redox cycles.

MeHg demethylation occurred in the control under moderately reducing to oxidizing E_H and low easily available organic matter. It needs to be further elucidated, if the limitation of electron donors leads to increased MeHg demethylation. Putative Hg demethylators were associated with various genera of Actinobacteria and nitrogen-fixing and nitrifying bacteria. Comprising methylotrophs and species with the demethylation gene *merA*, the genus *Hyphomicrobium* appeared to play an important role in the MeHg demethylating microbial community. Based on our findings, we recommend further studies dedicated to the demethylation potential of *Hyphomicrobium* assemblages combining culture-based methods and microbial community studies in environmental samples under moderately reducing redox conditions.

Environmental implication

Microbial-mediated transformation of mercury into methylmercury (MeHg) is hazardous for the environment and human health. Certain biochars can immobilize Hg in soils. However, regulating effects of biochar on Hg methylation and microbial community composition under fluctuating redox conditions is poorly understood. Therefore, we analyzed the microbial community in a Hg contaminated paddy soil non-treated and treated with rice hull biochar under controlled redox condition changes. Microbial assemblages were important in Hg transformation providing available organic matter and stimulating Hg methylation in the biochar-treated soil. In the non-treated soil, lower available organic matter fostered MeHg demethylation by Actinobacteria and nitrogen-fixing bacteria.

CRediT authorship contribution statement

Felizitas Boie: Data curation, Formal analysis, Investigation, Methodology, Visualization, Writing – original draft. **Jianxu Wang:** Funding acquisition, Writing – review & editing. **Thomas Ducey:** Formal analysis, Validation, Writing – review & editing. **Ying Xing:** Conceptualization, Writing – review & editing. **Jörg Rinklebe:** Writing – review & editing, Conceptualization, Funding acquisition, Investigation, Project administration, Resources, Software, Supervision, Validation.

Declaration of Competing Interest

The authors declare that they have no known competing financial interests or personal relationships that could have appeared to influence the work reported in this paper.

Data availability

Data will be made available on request.

Acknowledgements

We thank Hannah Rushmiller (Coastal Plains Soil, Water, Plant Research Center, U.S. Department of Agriculture) for conducting next-generation sequencing. Thanks go to the team of the Laboratory of Soil and Groundwater Management, University of Wuppertal, namely to Dipl.-Chem. Claus Vandenhirtz for chemical analyses, Christoph E. S. Kinder and Dr. Xing Yang for experimental support and to Dr. Christoph Weihrauch for intensive discussions on network analysis. Further, we want to thank two anonymous reviewers for their helpful comments.

Appendix A. Supporting information

Supplementary data associated with this article can be found in the online version at doi:10.1016/j.jhazmat.2024.134446.

References

[1] Xing, Y., Wang, J., Shaheen, S.M., Feng, X., Chen, Z., Zhang, H., Rinklebe, J., 2020. Mitigation of mercury accumulation in rice using rice hull-derived biochar as soil amendment: A field investigation. J Hazard Mater 388, 121747. https://doi.org/10.1016/j.jhazmat.2019.121747.

[2] Zhao, L., Meng, B., Feng, X., 2020. Mercury methylation in rice paddy and accumulation in rice plant: a review. Ecotoxicol Environ Saf 195, 110462. https://doi.org/10.1016/j.ecoenv.2020.110462.

[3] U.S. Environmental Protection Agency (1997): Mercury Study Report to Congress Volume VII: Characterization of human health and wildlife risks from mercury exposure in the United States. URL ⟨https://www.epa.gov/sites/default/files/2015–09/documents/volume7.pdf⟩.

[4] Guo, P., Rennenberg, H., Du, H., Wang, T., Gao, L., Flemetakis, E., Hänsch, R., Ma, M., Wang, D., 2023. Bacterial assemblages imply methylmercury production at the rice-soil system. Environ Int 178, 108066. https://doi.org/10.1016/j.envint.2023.108066.

[5] Regnell, O., Watras, C.J., 2019. Microbial mercury methylation in aquatic environments: a critical review of published field and laboratory studies. Environ Sci Technol 53, 4–19. https://doi.org/10.1021/acs.est.8b02709.

[6] Wang, J., Shaheen, S.M., Jing, M., Anderson, C.W.N., Swertz, A.-C., Wang, S.-L., Feng, X., Rinklebe, J., 2021. Mobilization, methylation, and demethylation of mercury in a paddy soil under systematic redox changes. Environ Sci Technol 55, 10133–10141. https://doi.org/10.1021/acs.est.0c07321.

[7] Bravo, A.G., Cosio, C., 2020. Biotic formation of methylmercury: a bio-physico-chemical conundrum. Limnol Oceanogr 65, 1010–1027. https://doi.org/10.1002/lno.11366.

[8] Ma, M., Du, H., Wang, D., 2019. Mercury methylation by anaerobic microorganisms: a review. Crit Rev Environ Sci Technol 49, 1893–1936. https://doi.org/10.1080/10643389.2019.1594517.

[9] Parks, J.M., Johs, A., Podar, M., Bridou, R., Hurt, R.A., Smith, S.D., Tomanicek, S. J., Qian, Y., Brown, S.D., Brandt, C.C., Palumbo, A.V., Smith, J.C., Wall, J.D., Elias, D.A., Liang, L., 2013. The genetic basis for bacterial mercury methylation. Science 339, 1332–1335. https://doi.org/10.1126/science.1230667.

[10] Gilmour, C.C., Podar, M., Bullock, A.L., Graham, A.M., Brown, S.D., Somenahally, A.C., Johs, A., Hurt, R.A., Bailey, K.L., Elias, D.A., 2013. Mercury methylation by novel microorganisms from new environments. Environ Sci Technol 47, 11810–11820. https://doi.org/10.1021/es403075t.

[11] Bravo, A.G., Peura, S., Buck, M., Ahmed, O., Mateos-Rivera, A., Herrero Ortega, S., Schaefer, J.K., Bouchet, S., Tolu, J., Björn, E., Bertilsson, S., 2018. Methanogens and iron-reducing bacteria: the overlooked members of mercury-methylating microbial communities in boreal lakes. Appl Environ Microbiol 84. https://doi.org/10.1128/AEM.01774-18.

[12] Liu, Y.-R., Johs, A., Bi, L., Lu, X., Hu, H.-W., Sun, D., He, J.-Z., Gu, B., 2018. Unraveling microbial communities associated with methylmercury production in paddy soils. Environ Sci Technol 52, 13110–13118. https://doi.org/10.1021/acs.est.8b03052.

[13] Yu, R.-Q., Barkay, T., 2022. Microbial mercury transformations: molecules, functions and organisms. Adv Appl Microbiol 118 31–90. https://doi.org/10.1016/bs.aambs.2022.03.001.

[14] Goñi-Urriza, M., Corsellis, Y., Lanceleur, L., Tessier, E., Gury, J., Monperrus, M., Guyoneaud, R., 2015. Relationships between bacterial energetic metabolism, mercury methylation potential, and hgcA/hgcB gene expression in Desulfovibrio dechloroacetivorans BerOc1. Environ Sci Pollut Res Int 22, 13764–13771. https://doi.org/10.1007/s11356-015-4273-5.

[15] Luo, H., Cheng, Q., He, D., Sun, J., Li, J., Pan, X., 2023. Recent advances in microbial mercury methylation: a review on methylation habitat, methylator, mechanism, and influencing factor. Process Saf Environ Prot 170, 286–296. https://doi.org/10.1016/j.psep.2022.12.007.

[16] Liu, Y.-R., Yang, Z., Zhou, X., Qu, X., Li, Z., Zhong, H., 2019. Overlooked role of putative Non-Hg methylators in predicting methylmercury production in paddy soils. Environ Sci Technol 53, 12330–12338. https://doi.org/10.1021/acs.est.9b03013.

[17] Barkay, T., Gu, B., 2022. Demethylation-the other side of the mercury methylation coin: a critical review. ACS Environ Au 2, 77–97. https://doi.org/10.1021/acsenvironau.1c00022.
[18] Zhou, X.-Q., Hao, Y.-Y., Gu, B., Feng, J., Liu, Y.-R., Huang, Q., 2020. Microbial communities associated with methylmercury degradation in paddy soils. Environ Sci Technol 54, 7952–7960. https://doi.org/10.1021/acs.est.0c00181.
[19] Figueiredo, N., Serralheiro, M.L., Canário, J., Duarte, A., Hintelmann, H., Carvalho, C., 2018. Evidence of mercury methylation and demethylation by the estuarine microbial communities obtained in stable Hg isotope studies. Int J Environ Res Public Health 15. https://doi.org/10.3390/ijerph15102141.
[20] Zhu, W., Song, Y., Adediran, G.A., Jiang, T., Reis, A.T., Pereira, E., Skyllberg, U., Björn, E., 2018. Mercury transformations in resuspended contaminated sediment controlled by redox conditions, chemical speciation and sources of organic matter. Geochim Et Cosmochim Acta 220, 158–179. https://doi.org/10.1016/j.gca.2017.09.045.
[21] Frohne, T., Rinklebe, J., Langer, U., Du Laing, G., Mothes, S., Wennrich, R., 2012. Biogeochemical factors affecting mercury methylation rate in two contaminated floodplain soils. Biogeosciences 9, 493–507. https://doi.org/10.5194/bg-9-493-2012.
[22] Liu, Y.-R., Yu, R.-Q., Zheng, Y.-M., He, J.-Z., 2014. Analysis of the microbial community structure by monitoring an Hg methylation gene (hgcA) in paddy soils along an Hg gradient. Appl Environ Microbiol 80, 2874–2879. https://doi.org/10.1128/AEM.04225-13.
[23] Pu, Q., Zhang, K., Poulain, A.J., Liu, J., Zhang, R., Abdelhafiz, M.A., Meng, B., Feng, X., 2022. Mercury drives microbial community assembly and ecosystem multifunctionality across a Hg contamination gradient in rice paddies. J Hazard Mater 435, 129055. https://doi.org/10.1016/j.jhazmat.2022.129055.
[24] Christensen, G.A., Somenahally, A.C., Moberly, J.G., Miller, C.M., King, A.J., Gilmour, C.C., Brown, S.D., Podar, M., Brandt, C.C., Brooks, S.C., Palumbo, A.V., Wall, J.D., Elias, D.A., 2018. Carbon amendments alter microbial community structure and net mercury methylation potential in sediments. Appl Environ Microbiol 84. https://doi.org/10.1128/AEM.01049-17.
[25] Liu, J., Lu, B., Poulain, A.J., Zhang, R., Zhang, T., Feng, X., Meng, B., 2022. The underappreciated role of natural organic matter bond Hg(II) and nanoparticulate HgS as substrates for methylation in paddy soils across a Hg concentration gradient. Environ Pollut 292, 118321. https://doi.org/10.1016/j.envpol.2021.118321.
[26] Bravo, A.G., Bouchet, S., Tolu, J., Björn, E., Mateos-Rivera, A., Bertilsson, S., 2017. Molecular composition of organic matter controls methylmercury formation in boreal lakes. Nat Commun 8, 14255. https://doi.org/10.1038/ncomms14255.
[27] He, M., Tian, L., Braaten, H.F.V., Wu, Q., Luo, J., Cai, L.-M., Meng, J.-H., Lin, Y., 2019. Mercury-organic matter interactions in soils and sediments: angel or devil? Bull Environ Contam Toxicol 102, 621–627. https://doi.org/10.1007/s00128-018-2523-1.
[28] Zhang, S., Wang, M., Liu, J., Tian, S., Yang, X., Xiao, G., Xu, G., Jiang, T., Wang, D., 2022. Biochar affects methylmercury production and bioaccumulation in paddy soils: Insights from soil-derived dissolved organic matter. J Environ Sci 119, 68–77. https://doi.org/10.1016/j.jes.2022.02.011.
[29] Yang, Q., Wang, Y., Zhong, H., 2021. Remediation of mercury-contaminated soils and sediments using biochar: a critical review. Biochar 3, 23–35. https://doi.org/10.1007/s42773-021-00087-1.
[30] Beckers, F., Awad, Y.M., Beiyuan, J., Abrigata, J., Mothes, S., Tsang, D.C.W., Ok, Y. S., Rinklebe, J., 2019. Impact of biochar on mobilization, methylation, and ethylation of mercury under dynamic redox conditions in a contaminated floodplain soil. Environ Int 127, 276–290. https://doi.org/10.1016/j.envint.2019.03.040.
[31] Beckers, F., Mothes, S., Abrigata, J., Zhao, J., Gao, Y., Rinklebe, J., 2019. Mobilization of mercury species under dynamic laboratory redox conditions in a contaminated floodplain soil as affected by biochar and sugar beet factory lime. Sci Total Environ 672, 604–617. https://doi.org/10.1016/j.scitotenv.2019.03.401.
[32] Xing, Y., Wang, J., Kinder, C.E.S., Yang, X., Slaný, M., Wang, B., Song, H., Shaheen, S.M., Leinweber, P., Rinklebe, J., 2022. Rice hull biochar enhances the mobilization and methylation of mercury in a soil under changing redox conditions: Implication for Hg risks management in paddy fields. Environ Int 168, 107484. https://doi.org/10.1016/j.envint.2022.107484.
[33] Chen, J., Sun, X., Li, L., Liu, X., Zhang, B., Zheng, J., Pan, G., 2016. Change in active microbial community structure, abundance and carbon cycling in an acid rice paddy soil with the addition of biochar. Eur J Soil Sci 67, 857–867. https://doi.org/10.1111/ejss.12388.
[34] Tang, Z., Zhang, L., He, N., Gong, D., Gao, H., Ma, Z., Fu, L., Zhao, M., Wang, H., Wang, C., Zheng, W., Zhang, W., 2021. Soil bacterial community as impacted by addition of rice straw and biochar. Sci Rep 11, 22185. https://doi.org/10.1038/s41598-021-99001-9.
[35] Tian, J., Wang, J., Dippold, M., Gao, Y., Blagodatskaya, E., Kuzyakov, Y., 2016. Biochar affects soil organic matter cycling and microbial functions but does not alter microbial community structure in a paddy soil. Sci Total Environ 556, 89–97. https://doi.org/10.1016/j.scitotenv.2016.03.010.
[36] Palansooriya, K.N., Wong, J.T.F., Hashimoto, Y., Huang, L., Rinklebe, J., Chang, S. X., Bolan, N., Wang, H., Ok, Y.S., 2019. Response of microbial communities to biochar-amended soils: a critical review. Biochar 1, 3–22. https://doi.org/10.1007/s42773-019-00009-2.
[37] Yu, K., Rinklebe, J., 2011. Advancement in soil microcosm apparatus for biogeochemical research. Ecol Eng 37, 2071–2075. https://doi.org/10.1016/j.ecoleng.2011.08.017.
[38] Liang, L., Horvat, M., Feng, X., Shang, L., Li, H., Pang, P., 2004. Re-evaluation of distillation and comparison with HNO3 leaching/solvent extraction for isolation of methylmercury compounds from sediment/soil samples. Appl Organomet Chem 18, 264–270. https://doi.org/10.1002/aoc.617.
[39] U.S. Environmental Protection Agency (1998): Method 1630: Methyl Mercury in Water by Distillation, Aqueous Ethylation, Purge and Trap, and Cold Vapor Atomic Fluorescence Spectrometry. URL ⟨https://www.epa.gov/sites/default/files/2015-08/documents/method_1630_1998.pdf⟩.
[40] Weishaar, J.L., Aiken, G.R., Bergamaschi, B.A., Fram, M.S., Fujii, R., Mopper, K., 2003. Evaluation of specific ultraviolet absorbance as an indicator of the chemical composition and reactivity of dissolved organic carbon. Environ Sci Technol 37, 4702–4708. https://doi.org/10.1021/es030360x.
[41] White, D.C., Davis, W.M., Nickels, J.S., King, J.D., Bobbie, R.J., 1979. Determination of the sedimentary microbial biomass by extractible lipid phosphate. Oecologia 40, 51–62. https://doi.org/10.1007/BF00388810.
[42] Frostegård, Å., Tunlid, A., Bååth, E., 1991. Microbial biomass measured as total lipid phosphate in soils of different organic content. J Microbiol Methods 14, 151–163. https://doi.org/10.1016/0167-7012(91)90018-L.
[43] Böhme, L., Langer, U., Böhme, F., 2005. Microbial biomass, enzyme activities and microbial community structure in two European long-term field experiments. Agric, Ecosyst Environ 109, 141–152. https://doi.org/10.1016/j.agee.2005.01.017.
[44] Rinklebe, J., Langer, U., 2008. Floodplain soils at the Elbe river, Germany, and their diverse microbial biomass. Arch Agron Soil Sci 54, 259–273. https://doi.org/10.1080/03650340701661206.
[45] Tatti, E., McKew, B.A., Whitby, C., Smith, C.J., 2016. Simultaneous DNA-RNA Extraction from Coastal Sediments and Quantification of 16S rRNA Genes and Transcripts by Real-time PCR. J Vis Exp. https://doi.org/10.3791/54067.
[46] Apprill, A., McNally, S., Parsons, R., Weber, L., 2015. Minor revision to V4 region SSU rRNA 806R gene primer greatly increases detection of SAR11 bacterioplankton. Aquat Microb Ecol 75, 129–137. https://doi.org/10.3354/ame01753.
[47] Parada, A.E., Needham, D.M., Fuhrman, J.A., 2016. Every base matters: assessing small subunit rRNA primers for marine microbiomes with mock communities, time series and global field samples. Environ Microbiol 18, 1403–1414. https://doi.org/10.1111/1462-2920.13023.
[48] Posit team, 2023. RStudio: Integrated Development Environment for R. Posit Software. PBC,, Boston, MA (URL). ⟨http://www.posit.co/⟩.
[49] Reddy, K.R., DeLaune, R.D., 2008. Biogeochemistry of Wetlands. CRC Press,.
[50] Bolan, S., Sharma, S., Mukherjee, S., Kumar, M., Rao, C.S., Nataraj, K.C., Singh, G., Vinu, A., Bhowmik, A., Sharma, H., El-Naggar, A., Chang, S.X., Hou, D., Rinklebe, J., Wang, H., Siddique, K.H.M., Abbott, L.K., Kirkham, M.B., Bolan, N., 2024. Biochar modulating soil biological health: a review. Sci Total Environ 914, 169585. https://doi.org/10.1016/j.scitotenv.2023.169585.
[51] Awad, Y.M., Ok, Y.S., Abrigata, J., Beiyuan, J., Beckers, F., Tsang, D.C., Rinklebe, J., 2018. Pine sawdust biomass and biochars at different pyrolysis temperatures change soil redox processes. Sci Total Environ 625, 147–154. https://doi.org/10.1016/j.scitotenv.2017.12.194.
[52] Ge, Y., Li, X., Palviainen, M., Zhou, X., Heinonsalo, J., Berninger, F., Pumpanen, J., Köster, K., Sun, H., 2023. Response of soil bacterial community to biochar application in a boreal pine forest. J Res 34, 749–759. https://doi.org/10.1007/s11676-022-01509-x.
[53] Kögel-Knabner, I., Amelung, W., Cao, Z., Fiedler, S., Frenzel, P., Jahn, R., Kalbitz, K., Kölbl, A., Schloter, M., 2010. Biogeochemistry of paddy soils. Geoderma 157, 1–14. https://doi.org/10.1016/j.geoderma.2010.03.009.
[54] Pett-Ridge, J., Silver, W.L., Firestone, M.K., 2006. Redox fluctuations frame microbial community impacts on n-cycling rates in a humid tropical forest soil. Biogeochemistry 81, 95–110. https://doi.org/10.1007/s10533-006-9032-8.
[55] Liu, P., Ptacek, C.J., Blowes, D.W., Finfrock, Y.Z., Gordon, R.A., 2017. Stabilization of mercury in sediment by using biochars under reducing conditions. J Hazard Mater 325, 120–128. https://doi.org/10.1016/j.jhazmat.2016.11.033.
[56] Peterson, B.D., Krabbenhoft, D.P., McMahon, K.D., Ogorek, J.M., Tate, M.T., Orem, W.H., Poulin, B.A., 2023. Environmental formation of methylmercury is controlled by synergy of inorganic mercury bioavailability and microbial mercury-methylation capacity. Environ Microbiol 25, 1409–1423. https://doi.org/10.1111/1462-2920.16364.
[57] LaRowe, D.E., van Cappellen, P., 2011. Degradation of natural organic matter: a thermodynamic analysis. Geochim Et Cosmochim Acta 75, 2030–2042. https://doi.org/10.1016/j.gca.2011.01.020.
[58] Zhang, L., Philben, M., Taş, N., Johs, A., Yang, Z., Wullschleger, S.D., Graham, D.E., Pierce, E.M., Gu, B., 2022. Unravelling biogeochemical drivers of methylmercury production in an Arctic fen soil and a bog soil. Environ Pollut 299, 118878. https://doi.org/10.1016/j.envpol.2022.118878.
[59] Liu, Y.-R., Zheng, Y.-M., Zhang, L.-M., He, J.-Z., 2014. Linkage between community diversity of sulfate-reducing microorganisms and methylmercury concentration in paddy soil. Environ Sci Pollut Res Int 21, 1339–1348. https://doi.org/10.1007/s11356-013-1973-6.
[60] Vishnivetskaya, T.A., Hu, H., van Nostrand, J.D., Wymore, A.M., Xu, X., Qiu, G., Feng, X., Zhou, J., Brown, S.D., Brandt, C.C., Podar, M., Gu, B., Elias, D.A., 2018. Microbial community structure with trends in methylation gene diversity and abundance in mercury-contaminated rice paddy soils in Guizhou, China. Environ Sci Process Impacts 20, 673–685. https://doi.org/10.1039/C7EM00558J.
[61] Liesack, W., 2000. Microbiology of flooded rice paddies. FEMS Microbiol Rev 24, 625–645. https://doi.org/10.1016/S0168-6445(00)00050-4.
[62] Wang, B., Hu, H., Bishop, K., Buck, M., Björn, E., Skyllberg, U., Nilsson, M.B., Bertilsson, S., Bravo, A.G., 2023. Microbial communities mediating net methylmercury formation along a trophic gradient in a peatland chronosequence. J Hazard Mater 442, 130057. https://doi.org/10.1016/j.jhazmat.2022.130057.

[63] Schaefer, J.K., Kronberg, R.-M., Björn, E., Skyllberg, U., 2020. Anaerobic guilds responsible for mercury methylation in boreal wetlands of varied trophic status serving as either a methylmercury source or sink. Environ Microbiol 22, 3685–3699. https://doi.org/10.1111/1462-2920.15134.
[64] Wang, L., O'Connor, D., Rinklebe, J., Ok, Y.S., Tsang, D.C.W., Shen, Z., Hou, D., 2020. Biochar aging: mechanisms, physicochemical changes, assessment, and implications for field applications. Environ Sci Technol 54, 14797–14814. https://doi.org/10.1021/acs.est.0c04033.
[65] Fierer, N., Bradford, M.A., Jackson, R.B., 2007. Toward an ecological classification of soil bacteria. Ecology 88, 1354–1364. https://doi.org/10.1890/05-1839.
[66] Drenovsky, R.E., Vo, D., Graham, K.J., Scow, K.M., 2004. Soil water content and organic carbon availability are major determinants of soil microbial community composition. Microb Ecol 48, 424–430. https://doi.org/10.1007/s00248-003-1063-2.
[67] Xu, M., Xia, H., Wu, J., Yang, G., Zhang, X., Peng, H., Yu, X., Li, L., Xiao, H., Qi, H., 2017. Shifts in the relative abundance of bacteria after wine-lees-derived biochar intervention in multi metal-contaminated paddy soil. Sci Total Environ 599-600, 1297–1307. https://doi.org/10.1016/j.scitotenv.2017.05.086.
[68] Kim, Y., Liesack, W., 2015. Differential assemblage of functional units in paddy soil microbiomes. PloS One 10, e0122221. https://doi.org/10.1371/journal.pone.0122221.
[69] Lingens, F., Blecher, R., Blecher, H., Blobel, F., Eberspacher, J., Frohner, C., Gorisch, H., Layh, G., 1985. Phenylobacterium immobile gen. nov., sp. nov., a Gram-Negative Bacterium That Degrades the Herbicide Chloridazon. Int J Syst Bacteriol 35, 26–39. https://doi.org/10.1099/00207713-35-1-26.
[70] Yang, S., Wen, X., Shi, Y., Liebner, S., Jin, H., Perfumo, A., 2016. Hydrocarbon degraders establish at the costs of microbial richness, abundance and keystone taxa after crude oil contamination in permafrost environments. Sci Rep 6, 37473. https://doi.org/10.1038/srep37473.
[71] Huffman, M.S., Madritch, M.D., 2018. Soil microbial response following wildfires in thermic oak-pine forests. Biol Fertil Soils 54, 985–997. https://doi.org/10.1007/s00374-018-1322-5.
[72] Lucas-Borja, M.E., Miralles, I., Ortega, R., Plaza-Álvarez, P.A., Gonzalez-Romero, J., Sagra, J., Soriano-Rodríguez, M., Certini, G., Moya, D., Heras, J., 2019. Immediate fire-induced changes in soil microbial community composition in an outdoor experimental controlled system. Sci Total Environ 696, 134033. https://doi.org/10.1016/j.scitotenv.2019.134033.
[73] Belova, S.E., Kulichevskaya, I.S., Akhmet'eva, N.P., Dedysh, S.N., 2014. Shifts in a bacterial community composition of a mesotrophic peatland after wildfire. Microbiology 83, 813–819. https://doi.org/10.1134/S0026261714060022.
[74] Ramana, C.V., Sasikala, C., Arunasri, K., Anil Kumar, P., Srinivas, T.N.R., Shivaji, S., Gupta, P., Süling, J., Imhoff, J.F., 2006. Rubrivivax benzoatilyticus sp. nov., an aromatic, hydrocarbon-degrading purple betaproteobacterium. Int J Syst Evolut Microbiol 56, 2157–2164. https://doi.org/10.1099/ijs.0.64209-0.
[75] Bao, P., Li, G.-X., 2017. Sulfur-driven iron reduction coupled to anaerobic ammonium oxidation. Environ Sci Technol 51, 6691–6698. https://doi.org/10.1021/acs.est.6b05971.
[76] Hu, X., Wang, J., Lv, Y., Liu, X., Zhong, J., Cui, X., Zhang, M., Ma, D., Yan, X., Zhu, X., 2021. Effects of heavy metals/metalloids and soil properties on microbial communities in farmland in the vicinity of a metals smelter. Front Microbiol 12, 707786. https://doi.org/10.3389/fmicb.2021.707786.
[77] Zhang, H., Zheng, X., Bai, N., Li, S., Zhang, J., Lv, W., 2019. Responses of soil bacterial and fungal communities to organic and conventional farming systems in East China. J Microbiol Biotechnol 29, 441–453. https://doi.org/10.4014/jmb.1809.09007.
[78] Qian, H., Hou, C., Liao, H., Wang, L., Han, S., Peng, S., Chen, W., Huang, Q., Luo, X., 2020. The species evenness of "prey" bacteria correlated with Bdellovibrio-and-like-organisms (BALOs) in the microbial network supports the biomass of BALOs in a paddy soil. FEMS Microbiol Ecol 96. https://doi.org/10.1093/femsec/fiaa195.
[79] Grady, E.N., MacDonald, J., Liu, L., Richman, A., Yuan, Z.-C., 2016. Current knowledge and perspectives of Paenibacillus: a review. Microb Cell Factor 15, 203. https://doi.org/10.1186/s12934-016-0603-7.
[80] Hirota, Y., Fujii, T., Sano, Y., Iyama, S., 1978. Nitrogen fixation in the rhizosphere of rice. Nature 276, 416–417. https://doi.org/10.1038/276416a0.
[81] Kloos, K., Fesefeldt, A., Gliesche, C.G., Bothe, H., 1995. DNA-probing indicates the occurrence of denitrification and nitrogen fixation genes in Hyphomicrobium. Distribution of denitrifying and nitrogen fixing isolates of Hyphomicrobium in a sewage treatment plant. FEMS Microbiol Ecol 18, 205–213. https://doi.org/10.1111/j.1574-6941.1995.tb00177.x.
[82] Kuypers, M.M.M., Marchant, H.K., Kartal, B., 2018. The microbial nitrogen-cycling network. Nat Rev Microbiol 16, 263–276. https://doi.org/10.1038/nrmicro.2018.9.